



Toward a universal carbonate clumped isotope calibration: Diverse synthesis and preparatory methods suggest a single temperature relationship

Julia R. Kelson^{a,*}, Katharine W. Huntington^{a,*}, Andrew J. Schauer^a,
Casey Saenger^{a,b}, Alex R. Lechler^c

^a Department of Earth and Space Sciences, University of Washington, 4000 15th Ave NE, Seattle, WA 98195, USA

^b Joint Institute for the Study of the Atmosphere and Ocean, University of Washington, 3737 Brooklyn Ave NE, Seattle, WA 98105, USA

^c Department of Geosciences, Pacific Lutheran University, Rieke Room 158, Tacoma, WA 98447, USA

Received 22 April 2016; accepted in revised form 16 October 2016; Available online 21 October 2016

Abstract

Carbonate clumped isotope (Δ_{47}) thermometry has been applied to a wide range of problems in earth, ocean and biological sciences over the last decade, but is still plagued by discrepancies among empirical calibrations that show a range of Δ_{47} -temperature sensitivities. The most commonly suggested causes of these discrepancies are the method of mineral precipitation and analytical differences, including the temperature of phosphoric acid used to digest carbonates. However, these mechanisms have yet to be tested in a consistent analytical setting, which makes it difficult to isolate the cause(s) of discrepancies and to evaluate which synthetic calibration is most appropriate for natural samples. Here, we systematically explore the impact of synthetic carbonate precipitation by replicating precipitation experiments of previous workers under a constant analytical setting. We (1) precipitate 56 synthetic carbonates at temperatures of 4–85 °C using different procedures to degas CO_2 , with and without the use of the enzyme carbonic anhydrase (CA) to promote rapid dissolved inorganic carbon (DIC) equilibration; (2) digest samples in phosphoric acid at both 90 °C and 25 °C; and (3) hold constant all analytical methods including acid preparation, CO_2 purification, and mass spectrometry; and (4) reduce our data with ^{17}O corrections that are appropriate for our samples. We find that the CO_2 degassing method does not influence Δ_{47} values of these synthetic carbonates, and therefore probably only influences natural samples with very rapid degassing rates, like speleothems that precipitate out of drip solution with high $p\text{CO}_2$. CA in solution does not influence Δ_{47} values in this work, suggesting that disequilibrium in the DIC pool is negligible. We also find the Δ_{47} values of samples reacted in 25 and 90 °C acid are within error of each other (once corrected with a constant acid fractionation factor). Taken together, our results show that the Δ_{47} -temperature relationship does not measurably change with either the precipitation methods used in this study or acid digestion temperature. This leaves phosphoric acid preparation, CO_2 gas purification, and/or data reduction methods as the possible sources of the discrepancy among published calibrations. In particular, the use of appropriate ^{17}O corrections has the potential to reduce disagreement among calibrations. Our study nearly doubles the available synthetic carbonate calibration data for Δ_{47} thermometry (adding 56 samples to the 74 previously published samples). This large population size creates a robust calibration that enables us to examine the potential for calibration slope aliasing due to small sample size. The similarity of Δ_{47} values among carbonates precipitated under such diverse conditions suggests that many natural samples grown at 4–85 °C in moderate pH conditions (6–10) may also be described by our Δ_{47} -temperature relationship.

© 2016 Elsevier Ltd. All rights reserved.

* Corresponding authors.

E-mail addresses: jrkelson@uw.edu (J.R. Kelson), katel@uw.edu (K.W. Huntington).

Keywords: Clumped isotopes; Oxygen isotopes; Paleothermometer calibration; Carbonate precipitation

1. INTRODUCTION

Carbonate clumped isotope (Δ_{47}) thermometry is applied to an increasing range of natural systems, contributing to discoveries in areas such as paleoclimate, paleoaltimetry, and basinal fluid migration (e.g., see reviews of Eiler, 2007, 2011; Affek, 2012; Eiler et al., 2013, 2014; Huntington and Lechler, 2015). Δ_{47} thermometry estimates mineral growth temperature using the thermodynamic tendency for ^{13}C and ^{18}O to bond in carbonate molecules at lower temperatures (e.g., Schauble et al., 2006). The Δ_{47} value of CO_2 , derived from phosphoric acid digestion of carbonate minerals, measures the abundance of ^{13}C and ^{18}O in the same molecule in excess of what would occur by random chance (Ghosh et al., 2006; Schauble et al., 2006). The temperature dependence of ^{13}C – ^{18}O clumping in carbonates has been studied from a theoretical perspective (Schauble et al., 2006; Guo et al., 2009; Passey and Henkes, 2012; Hill et al., 2014; Tripathi et al., 2015). However, given the as of yet imperfect knowledge of carbonate precipitation processes, acid fractionation effects, and analytical artifacts, accurate empirical Δ_{47} -temperature calibrations are necessary to apply the thermometer with confidence. Many empirical calibrations have been published based on analyses of carbonates with known growth temperatures, including synthetic carbonates (Ghosh et al., 2006; Dennis and Schrag, 2010; Daëron et al., 2011; Passey and Henkes, 2012; Zaarur et al., 2013; Fernandez et al., 2014; Tang et al., 2014; Defliese et al., 2015; Kluge et al., 2015; Tripathi et al., 2015) and natural biogenic and abiogenic carbonates (Ghosh et al., 2007; Eagle et al., 2010, 2013, 2015; Tripathi et al., 2010, 2015; Thiagarajan et al., 2011; Saenger et al., 2012; Henkes et al., 2013; Grauel et al., 2013; Came et al., 2014; Wacker et al., 2014; Petrizzo et al., 2014; Kele et al., 2015).

Despite the extensive body of research on calibrating the Δ_{47} thermometer, unresolved discrepancies of up to 10–15 °C exist among published empirical calibrations (Table 2). The first two published synthetic calcite calibrations differ in their temperature sensitivity: Ghosh et al. (2006) report a steep Δ_{47} -temperature slope ($m = 0.0636 \times 10^6/\text{T}^2$), while Dennis and Schrag (2010) report a relatively shallower slope ($m = 0.0362 \times 10^6/\text{T}^2$) (both slopes as reported in the absolute reference frame in Dennis et al. (2011)). More recent calibrations have slopes that fall between these two end-members, such that a spectrum of temperature sensitivities has been published (Table 2). These discrepancies in slope and resulting temperature estimates are large enough to significantly change interpretations of Δ_{47} measured in natural samples. Yet it is unclear if these calibrations disagree because of true differences in the Δ_{47} values of carbonates synthesized or because of differences in laboratory analysis methods.

Previous workers have suggested that calibrations diverge because different carbonate precipitation methods cause calibration samples to have Δ_{47} values that reflect

variables other than growth temperature (e.g. Dennis and Schrag, 2010; Dennis et al., 2011; Henkes et al., 2013; Zaarur et al., 2013; Fernandez et al., 2014; Tang et al., 2014). Most notably, opposing views have been expressed about which method of CO_2 degassing during synthetic calcite growth (passive degassing or active degassing with N_2 , sensu Kim and O'Neil (1997) and Dennis and Schrag (2010)) favors clumped isotope disequilibrium (Affek and Zaarur, 2014; cf. Fernandez et al., 2014). Recent publications have shown that Δ_{47} values can also be influenced by growth rate, pH, and DIC disequilibrium (Hill et al., 2014; Tang et al., 2014; Watkins and Hunt, 2015; Tripathi et al., 2015).

However, the influence of carbonate precipitation methods used by previous workers to create empirical Δ_{47} -temperature calibrations remains to be systematically evaluated in a single analytical setting, making it difficult to determine if calibration discrepancies arise due to differences in carbonate precipitation techniques or analysis techniques. Differences in analysis methods that could cause calibrations to diverge could occur at multiple steps in the sample preparation and measurement process including: digestion of the carbonate sample to produce CO_2 gas for analysis (e.g., Wacker et al., 2013, 2014; Fernandez et al., 2014; Came et al., 2014; Petrizzo et al., 2014; Defliese et al., 2015), sample gas purification, data processing and absolute reference frame construction (Dennis et al., 2011; Daëron et al., 2016; Olack and Colman, 2016; Schauer et al., 2016), or background measurements (He et al., 2012; Bernasconi et al., 2013; Fiebig et al., 2015).

Here, we systematically explore the influence of carbonate precipitation methods on Δ_{47} values. We precipitate carbonate at known temperatures using various methods, including the methods used in previously published synthetic carbonate clumped isotope calibrations over the temperature range 4–85 °C. We then digest samples in phosphoric acid at both 90 °C and 25 °C, but control for other preparatory and analytical variables by purifying and measuring the resulting CO_2 using identical procedures. Our results support previous findings that rule out acid digestion temperature as the cause of the calibration discrepancies (Defliese et al., 2015). Most importantly, our large dataset (56 samples; 200 individual sample analyses bracketed by extensive equilibrated CO_2 and carbonate standard measurements) shows that synthetic carbonate precipitation methods are unlikely to be responsible for previous calibration discrepancies. Furthermore, we define a robust Δ_{47} -temperature calibration that is appropriate for estimating temperature from natural, abiogenic carbonates precipitated via a variety of pathways. Our findings point toward specific analytical and data correction methods that contribute to discrepancies among previous calibrations, including ^{17}O corrections (Daëron et al., 2016; Olack and Colman, 2016; Schauer et al., 2016). Normalizing these methods across laboratories will be required to decrease dispersion among calibration data and correctly interpret

Δ_{47} data across the broad range of research questions to which they are applied.

2. MATERIALS AND METHODS

We investigate how precipitation methods can influence Δ_{47} values by replicating techniques used in previous synthetic carbonate Δ_{47} calibration studies at temperatures <100 °C. We conduct experiments with and without the use of a bovine enzyme carbonic anhydrase (CA); measure solution pH and isotopic composition at the start and end of each experiment; confirm sample mineralogy with XRD; measure mineral grain size with microprobe imaging; measure carbonate isotopic composition; and evaluate the fractionation that occurs during phosphoric acid reactions at 25 and 90 °C. All analytical, reference frame, and data reduction methods except the acid digestion procedure were held constant to facilitate direct comparison of carbonate precipitation methods.

2.1. Carbonate precipitation methods

We grew carbonates at known temperatures of 4–85 °C using precipitation methods chosen to replicate the previous calibration studies of [Dennis and Schrag \(2010\)](#), [Zaarur et al. \(2013\)](#), [Ghosh et al. \(2006\)](#), and [Kim and O'Neil \(1997\)](#) in a consistent analytical setting. We assume that by replicating the methods used in these previous studies we replicate to the extent possible the conditions that control kinetics of DIC equilibration and carbonate precipitation. In addition to replicating these previously published experiments, we conducted additional experiments to isolate the effects of specific variables (e.g., concentration of salts, and catalyzing DIC equilibration).

In all experiments, solutions were placed in an Erlenmeyer flask and allowed to thermally equilibrate in a temperature-controlled oil bath or refrigerator. The temperature was continuously logged with a thermocouple (Campbell Scientific data logger CR10X with thermocouple type T or an Onset Hobo U-Series data logger with a TMC1-HD temperature sensor, manufacturer's accuracy of ± 0.5 °C). The thermocouples were calibrated to the freezing and boiling points of water. The standard deviation of hot plate temperature was ± 0.7 °C, while that of the refrigerators (4 and 8 °C experiments) was ± 0.2 °C.

Synthetic calcium carbonates were precipitated (1) by combining NaHCO_3 and CaCl_2 in solution (e.g. [Kim and O'Neil, 1997](#); [Dennis and Schrag, 2010](#)) or (2) by dissolving CaCO_3 in water whose pH had been lowered by CO_2 bubbling, and then filtering out un-dissolved crystals (e.g., [Kim and O'Neil, 1997](#); and [Zaarur et al., 2013](#)). The NaHCO_3 used in the experiments had a $\delta^{13}\text{C}$ value of -3.3‰ (VPDB, measured using a Kiel III carbonate device coupled to a Finnegan DeltaPlus Isotope Ratio Mass Spectrometer). The CO_2 gas that was bubbled through the experimental solutions had a $\delta^{13}\text{C}$ value of -36.5‰ (VPDB). CO_2 was removed from solution, which increased its pH and saturation state, causing carbonate to precipitate. CO_2 was removed either actively by bubbling N_2 through solutions (e.g., [Ghosh et al., 2006](#); [Zaarur et al., 2013](#)), or passively

by allowing CO_2 to degas into the atmosphere (e.g., [Dennis and Schrag, 2010](#); [Affek and Zaarur, 2014](#)). As in previous studies, the solution was not stored before degassing was initiated in any of the methods (i.e., no DIC equilibration time allowed prior to degassing).

Experiments were allowed to proceed until enough material for Δ_{47} analysis precipitated; about one week for higher temperature samples and up to six weeks for lower temperature samples. All sample types were collected with a rubber spatula and were vacuum filtered from solution (Whatman #40 8 μm filter paper). The samples were freeze-dried overnight prior to acid digestion, purification and analysis. [Table 1](#) provides the names and a detailed comparison of the precipitation methods used in this work.

In two of the filtered crystal method experiments ([Table 1](#)), we observed thin films of carbonate floating on the air–water interface. Previous experiments that did not stir the solution (unlike our filtered crystal experiments, which were stirred gently with N_2 bubbles) also observed floating carbonates, and because of their morphology, called them rafts ([Affek and Zaarur, 2014](#)). These rafts likely formed when they experienced rapid CO_2 degassing at the surface ([Affek and Zaarur, 2014](#)). We collected the raft morphology material and analyzed it separately from other precipitate material.

In several experiments, we added the enzyme CA before the addition of salts in order to promote isotopic equilibrium among the DIC species ([Table A1](#)). [Uchikawa and Zeebe \(2012\)](#) found that at 25 °C and pH of 8.3, CA reduces the time it takes DIC species reach isotopic equilibrium from ~ 600 min to less than 200 min. CA has previously been used in carbonate synthesis experiments ([Watkins et al., 2013, 2014](#); [Tripathi et al., 2015](#)). CA is most active at 60 °C, and fully inactive above 80 °C ([DeLuca et al., 2013](#)). We determined that the CA was working in our experimental conditions by measuring the isotopic composition of CO_2 gas as it equilibrated at room temperature with a solution identical to our precipitation solution. CO_2 gas approached oxygen isotopic equilibrium faster when CA was in solution (equilibration rate of 0.45‰/minute with CA, as opposed to a rate of 0.30‰/minute) ([Fig. S1](#)).

We also analyzed an eggshell from a domestic chicken. We use the body temperature of a chicken (42 °C, [Randall and Hiestand, 1939](#)) to represent the growth temperature of the shell material ([Wacker et al., 2014](#); [Eagle et al., 2015](#)).

2.2. Mineralogy and grain size analytical methods

Samples were analyzed for their mineralogy using a Bruker F8 Focus Powder X-Ray Diffractometer at the Materials Sciences Department at the University of Washington. The spectral signatures were analyzed using JADE™ software and mineral database. Grain size of select calcite samples was measured using imagery of the samples as described by [Tobin et al. \(2011\)](#). The images were taken with a JEOL 733 electron microprobe using secondary and backscattered electron signals ([Fig. S3](#)). The 50th percentile (d50) grain size is considered the representative grain size.

Table 1
Synthetic carbonate precipitation methods used in this work.

Method	“Active degassing”	“Passive degassing”	“Mixed solution”	“Filtered crystal”
Citation replicated	Kim and O’Neil (1997)	Modified after Kim and O’Neil (1997), Dennis and Schrag (2010) ^a	Dennis and Schrag (2010)	Zaarur et al. (2013), Ghosh et al. (2006)
Adding reagents	CO ₂ bubbled for 10 min, NaHCO ₃ was added, CO ₂ bubbled for an additional 10 min, CaCl ₂ *2H ₂ O was added, CO ₂ was bubbled for an additional 10 min	CO ₂ bubbled for 10 min, NaHCO ₃ was added, CO ₂ bubbled for an additional 10 min, CaCl ₂ *2H ₂ O was added, CO ₂ was bubbled for an additional 10 min	Thermally equilibrated solutions of NaHCO ₃ and CaCl ₂ *2H ₂ O were slowly combined in ~5 mL quantities	CO ₂ bubbled for 1 hour, then 1 g of in-house calcite standard, C64, was added. CO ₂ bubbled until CaCO ₃ dissolved
CA added?	After salts were added, in some experiments (Table A1)	After salts were added, in some experiments (Table A1)	After solutions were combined, in some experiments (Table A1)	No
Filtering	NA	NA	NA	Filtered with Whatman #40 8 μm filter paper
Stirring	Magnetic stir bar	Magnetic stir bar	Magnetic stir bar	N ₂ bubbles
Degassing	N ₂ bubbled (20 bubbles/30 seconds) with a pasteur pipe to actively degas CO ₂	CO ₂ allowed to passively degas into the atmosphere, through 1 hole at the top of the beaker	CO ₂ allowed to passively degas into the atmosphere, through 1 hole at the top of the beaker	N ₂ bubbling (20 bubbles/30 seconds) with a pasteur pipe to actively degas CO ₂
Carbonate observation	In suspension and coating the bottom of the flask	In suspension and coating the bottom of the flask	Attached to the bottom of the flask (had to be scraped aggressively to remove)	Coating the bottom of the flask and floating rafts

^a This method does not strictly replicate either Kim and O’Neil (1997) or Dennis and Schrag (2010). Kim and O’Neil (1997)/the “active degassing” method bubbled both N₂ and CO₂, while Dennis and Schrag (2010)/ the “mixed solution method” bubble neither. This method only bubbles CO₂ in order to isolate the influence of bubbling CO₂ in solution. Additionally, we have varied the stoichiometry and ionic concentrations in some of these samples (Table A1).

2.3. Stable isotope analytical methods

2.3.1. Measurements of $\delta^{18}O$ and pH of solution

The solution from which the calcium carbonates precipitated was sampled for water $\delta^{18}O$ and pH measurements at the start and end of each experiment. pH was measured using a Mettler Toledo FG2 FiveGo Portable pH meter (pH accuracy quoted by the manufacturer of ± 0.01). Water $\delta^{18}O$ was measured at the University of Washington IsoLab using a Picarro L2120i wavelength-scanned cavity ring-down spectrometer (Gupta et al., 2009). Water samples were referenced to the VSMOW scale using two bracketing internal reference waters that were measured against VSMOW and SLAP using GISP as a quality control reference.

2.3.2. Measurements of Δ_{47} , $\delta^{18}O$, and $\delta^{13}C$ of calcium carbonates

Clumped, carbon, and oxygen isotopic compositions of the calcium carbonate samples were measured at the University of Washington IsoLab. The details of the automated vacuum line and sample purification methods used in IsoLab are described in Burgener et al. (2016). In this work, 6–9 mg of sample were reacted for 10 min in a common bath of 90 °C phosphoric acid with a starting specific gravity of 1.904–1.970 g/cm³ (multiple batches of acid were used throughout the course of this work). Some samples were also reacted overnight at 25 °C in McCrea-type reaction vessels (McCrea, 1950) with 1.5–2 mL of the same phosphoric acid.

A solid calcium carbonate reference material was run for every ~4 sample unknowns including: NBS19, three in-house calcites with disparate bulk compositions (C64 and C2, both reagent-grade; and Coral, a tropical *Porites* coral sample). C64 was also reacted in 25 °C phosphoric acid and purified then analyzed with the samples reacted at 25 °C. Apart from monitoring Δ_{47} , standards C64, C2, and Coral were used to place all $\delta^{13}C$ and $\delta^{18}O$ values on the VPDB scale (see data reduction code in Schauer et al., 2016). These three materials have been calibrated to NBS19, LSVEC, and NBS18 using a Kiel III Carbonate device coupled to Finnegan DeltaPlus Isotope Ratio Mass Spectrometer. The values of our calcium carbonate standards can be found in the Tables S2, S4, S6, and S7.

Purified CO₂ break seals were placed on an automated 10-port tube cracker inlet system on a Thermo MAT 253 configured to measure m/z 44–49 inclusive. To start each sample analysis, sample and reference gas bellows were fully expanded and evacuated. Sample gas was filled into the sample bellows and pressure was measured. Reference gas bellows were automatically filled to a pressure equal to the sample bellows pressure (this is done by modifying the sample introduction and reference refill scripts as described in Schauer et al., 2016). The CO₂ reference gas is from a corn fermentation plant ($\delta^{13}C$ –10.2‰, $\delta^{18}O$ –6.0‰, versus NBS-19). Sample and reference signals were balanced on m/z 47 to a signal of 2.55 V from installation of the MAT 253 until April 2015 (as recommended by Thermo because of irreconcilable noise issues). After April 2015 Thermo installed a newly designed amplifier power supply

and we began pressure balancing on m/z 44 to a signal of 16 V (approximately 2.55 V on m/z 47). Pressure base line (PBL) was automatically measured while CO_2 is flowing at 80 V left of peak center before each sample measurement (similar to He et al., 2012; code in Schauer et al., 2016). Our background measurement is used instead of the default Iso-Dat background, and all V signals (44–49) are corrected for the background before they are output (code in Schauer et al., 2016). Sample CO_2 m/z 44–49 were measured against reference CO_2 for 6 acquisitions of 10 sample-reference comparisons cycles with 26-second integration times, for a total of 1560 seconds of counting. Standard amplifications were used for m/z 44–46 (3×10^8 , 3×10^{10} , 1×10^{11} Ω , respectively); m/z 47–49 were measured with 1×10^{12} Ω amplification. After the 6 sample-reference comparison cycles, water backgrounds were measured by peak centering on m/z 18 of both sample and reference.

Δ_{47} was calculated using previously established methods (Eiler and Schauble, 2004; Afek and Eiler, 2006; Huntington et al., 2009; Dennis et al., 2011), with the exception of ^{17}O abundance correction values. The λ (0.528) and K (0.01022461) values recommended by Brand et al. (2010) were used to correct for ^{17}O interference in $\delta^{13}\text{C}$ measurements made with a mass spectrometer (Daëron et al., 2016; Schauer et al., 2016). Traditionally, the ^{17}O parameters that are used to calculate Δ_{47} values come from Huntington et al. (2009), which are indistinguishable from those of Santrock et al. (1985). The Brand et al. (2010) values are likely more appropriate than the Santrock et al. (1985) values for most natural and synthetic samples because they are based on measurements of meteoric water, rather than meteorites (Schauer et al., 2016). Additionally, using the Brand et al. (2010) parameters minimizes an apparent dependency of Δ_{47} on $\delta^{13}\text{C}$, as described in Schauer et al. (2016). Δ_{47} values are corrected for their dependence on δ_{47} with the slope of the reference frame gases, then projected into the absolute reference frame (ARF) (Dennis et al., 2011). Our reference frame gases are made by heating CO_2 in a quartz break seal to 1000 °C, or by equilibrating CO_2 with water of various isotopic compositions at 4 and 60 °C in a Pyrex break seal (Tables S1, S3, and S5). The heated and equilibrated gases were purified using the same vacuum line and method as the carbonate-derived CO_2 samples, and were measured regularly throughout the period of analysis.

Samples that were reacted at 90 °C are presented without an acid fractionation factor (AFF) (i.e., they are presented in the ‘90 °C reference frame’). When projecting samples into the 25 °C reference frame for comparison purposes in this paper, we used an AFF of 0.082‰ (Defiense et al., 2015). The Defiense et al. (2015) AFF is within error of the value we calculate based on a smaller dataset from this study, but we choose to use the more robust Defiense et al. (2015) AFF because their value is based on a large number of replicates of many samples with diverse compositions reacted at different temperatures.

The data span three distinct reference frames, each continually constructed with reference gases during the analysis period. The break between the first and second reference frames was established because the stainless steel tubing

of the cryogenic traps was replaced with nickel tubing to reduce water contamination in the vacuum line. The break between the second and third reference frames was established in April 2015 because we started to pressure balance on m/z 44 instead of m/z 47. The Δ_{47} values of the calcium carbonate standards measured in these three reference frames are indistinguishable within measurement error (Tables S2, S4, S6).

Peirce’s criterion was used to identify and remove data outliers (Ross, 2003; Zaarur et al., 2013); 7 out of 207 total analyses were removed. The average Δ_{47} internal mass spectrometer uncertainty is $\sim 0.008\%$, and the total internal uncertainty due to both the mass spectrometer and the projection into the reference frame for each replicate is 0.012‰ on average (code in Schauer et al., 2016). External reproducibility, which we calculate as the standard deviation of replicates, is usually larger ($\sim 0.015\%$), so we report that larger uncertainty. The final uncertainty that we report for samples is the standard error, calculated as the larger value between (1) the standard deviation of all C64 replicates for the relevant reference frame divided by the square root of the number of sample replicates, or (2) the standard deviation of the sample replicates divided by the square root of the number of sample replicates. We use C64 to represent error because it is the laboratory standard that was analyzed most regularly, and is a homogenous material that allows us to monitor long-term errors of our methods.

An ordinary least squares regression is used to calculate linear regressions. A model II regression that considers the errors in both the predictor and response variables (i.e., York et al., 2004) is not needed because the error in our solution temperature measurements is relatively small (Wacker et al., 2014).

3. RESULTS

3.1. Solution chemistry, mineralogy, and grain size

Details of each precipitation experiment can be found in Table A1. pH values at the start of experiments range from 5.36 to 8.77. pH values at the end of experiments range from 5.84 to 8.73 (Table A1). The average increase in pH from start to end of experiment is 0.5 (an average change in pH of 9%). The $\delta^{18}\text{O}$ of Seattle DI tap water is -10.5% (VSMOW), and the measured $\delta^{18}\text{O}$ of the solutions was close to this value. Minimal evaporation occurred during precipitation experiments, and the $\delta^{18}\text{O}$ of the solution did not change significantly.

XRD analyses confirm that most of the samples precipitated are 100% calcite. Some of the higher temperature samples are aragonite or some mixture of calcium carbonate polymorphs (Table A1). Our non-calcite samples are within measurement error (1 standard error, SE) of calcite samples grown at the same temperature (Fig. S2), consistent with recent work by Defiense et al. (2015) showing that mineralogy does not measurably influence the Δ_{47} values, despite theoretical calculations to the contrary (Guo et al., 2009). Linear regressions through the calcite-only sample types are within one standard error of regressions through all samples (Table 2). Therefore, we have included

Table 2
Synthetic and abiogenic Δ_{47} -temperature calibrations.

Regression	Slope $\times 10^6/T^2 \pm 1$ SE	Intercept ± 1 SE	r^2	Acid Dig. T °C (AFF) ^a	Calib. Range °C	n (samples)
<i>This work – all samples digested in 90 °C acid</i>						
Actively degassed	0.0396 \pm 0.0035	0.155 \pm 0.035	0.921	90 (0)	6 to 80	13
Passively degassed	0.0412 \pm 0.0018	0.139 \pm 0.019	0.970	90 (0)	6 to 80	18
Mixed solution	0.0429 \pm 0.0020	0.132 \pm 0.021	0.967	90 (0)	6 to 85	18
Filtered	0.0384 \pm 0.0063	0.179 \pm 0.073	0.924	90 (0)	4 to 50	5
All sample types (Eq. (1))	0.0417 \pm 0.0013	0.139 \pm 0.014	0.95	90 (0)	4 to 85	56
<i>This work – calcite only, samples digested in 90 °C acid</i>						
Actively degassed	0.0372 \pm 0.0047	0.183 \pm 0.050	0.887	90 (0)	6 to 77	10
Passively degassed	0.0407 \pm 0.0019	0.144 \pm 0.021	0.975	90 (0)	6 to 78	12
Mixed solution	0.0420 \pm 0.0028	0.142 \pm 0.032	0.957	90 (0)	6 to 55	12
all sample types	0.0408 \pm 0.0017	0.148 \pm 0.019	0.941	90 (0)	4 to 78	38
<i>This work – samples digested in 25 °C acid</i>						
Actively degassed	0.0383 \pm 0.0041	0.266 \pm 0.042	0.966	25 (0)	6 to 80	5
Passively degassed	0.0327 \pm 0	0.313 \pm 0	NaN	25 (0)	23 to 48	2
Mixed solution	0.0447 \pm 0.0052	0.209 \pm 0.054	0.974	25 (0)	6 to 80	4
All sample types	0.0407 \pm 0.0030	0.242 \pm 0.031	0.95	25 (0)	6 to 77	11
<i>Synthetic & Abiogenic Calibrations (in order of shallow to steep slope)</i>						
Wacker et al. (2014)	0.0327 \pm 0.0026	0.303 \pm 0.03	0.9915	90 (0.069)	9 to 38	7
Defliese et al. (2015)	0.0348 \pm 0.00229	0.3031 \pm 0.0244	0.8778	75 (0.067)	5 to 70	8
Dennis and Schrag (2010) ^b	0.0362 \pm 0.0018	0.292 \pm 0.0194		90 (0.081)	7.5 to 77	15
Kluge et al. (2015)	0.038 \pm 0.007	0.259 \pm 0.006		70/90 (various)	23 to 250	29
Tang et al. (2014)	0.0387 \pm 0.0072	0.2532 \pm 0.0829		90 & 100	5 to 40	23
Kele et al. (2015)	0.044 \pm 0.005	0.205 \pm 0.47	0.96	70 (0.064)	5.6 to 95	25
Tripati et al. (2015), excluding low T	0.046 \pm 0.0074	0.1649 \pm 0.0786		90 (0.092)	25 to 50	10
Affek and Zaarur (2014)	0.048 \pm 0.0028	0.2149 \pm 0.0295	0.84	25 (0)	7 to 69	14
Tripati et al. (2015)	0.0505 \pm 0.0034	0.1185 \pm 0.038		90 (0.092)	0.5 to 50	12
Zaarur et al. (2013)	0.0526 \pm 0.0025	0.052 \pm 0.0284	0.93	25 (0)	1 to 60	14
Ghosh et al. (2006) ^b	0.0636 \pm 0.0049	0.005 \pm 0.062		25 (0)	1 to 50	7

^a Values in parenthesis are the acid fractionation factors used by the studies' authors to calculate the calibration.

^b Values recalculated in Dennis et al. (2011).

the non-calcite samples for the purpose of drawing more robust conclusions over larger temperature ranges.

Grain size d50 values of the subset of synthetic calcites analyzed range from 2.8 to 9.0 μm . Aragonite samples display the expected needle-like structure, and therefore are not included in the grain size comparison (Fig. S3). Each calcite sample has grains of uniform size (standard deviation of 2–3 μm). In samples that were measured, grain size does not vary systematically with growth temperature.

3.2. Stable isotope values of synthetic calcium carbonates

200 total individual analyses of 56 synthetic calcium carbonates were performed. 166 analyses were conducted by digesting each of the 56 samples in 90 °C acid for a total of 2–4 replicates per sample. 34 analyses were conducted by digesting 11 of the total 56 samples in 25 °C acid for a total of 2–4 replicates per sample. At least 3 replicates per sample were performed, unless insufficient material limited our number of replicates.

The $\delta^{13}\text{C}$ values (VPDB) of the samples range from 1.6 to -25.7‰ with an average standard error (SE) of 0.13 ‰ . The $\delta^{18}\text{O}$ values (VPDB) of samples range from -6.5 to -20.8‰ with an average SE of 0.08 ‰ (Table A1). The regressions for mineral–water oxygen isotope fractionation versus temperature for the different sample types are statistically the same; an ancova analysis accepts the null hypothesis ($p = 0.12$ and greater).

The Δ_{47} values of samples reacted at 90 °C range from 0.457 to 0.691 ‰ with an average SE of 0.015 ‰ on replicate analyses of the same sample (no AFF applied). The Δ_{47} values of samples reacted at 25 °C range from 0.558 to 0.792 ‰ with an average SE of 0.014 ‰ (no AFF applied) (Fig 3).

The samples grown with and without CA for a given growth temperature have Δ_{47} and $\delta^{18}\text{O}$ water–calcite fractionation values that are the same within measurement uncertainty (1 SE) (Fig. 1, Fig. 2, Table A2). A t-test accepts the null hypothesis that the sample populations with CA and without CA have the same mean Δ_{47} values ($p = 0.81$). Our results show that CA does not influence Δ_{47} even at optimum enzyme temperatures (<80 °C) (Fig. 1). For the rest of this paper, the samples with CA ($n = 13$) are grouped with samples without CA when discussing Δ_{47} -temperature relationships.

The Δ_{47} of samples grown with different methods at approximately the same temperature are indistinguishable from one another within measurement error (1 SE) (Fig. 4). The different sample populations are not statistically different (null hypothesis of the t-test accepted at 95% confidence level for all comparisons). The slope and intercept values of the regression through each of the sample types are within error of the others (Table 2). An analysis of covariance (ancova) test also accepts the null hypothesis that the linear regressions are the same at the 95% confidence level ($p = 0.21$ and greater). When the Δ_{47} of samples grown at nominally the same temperature using

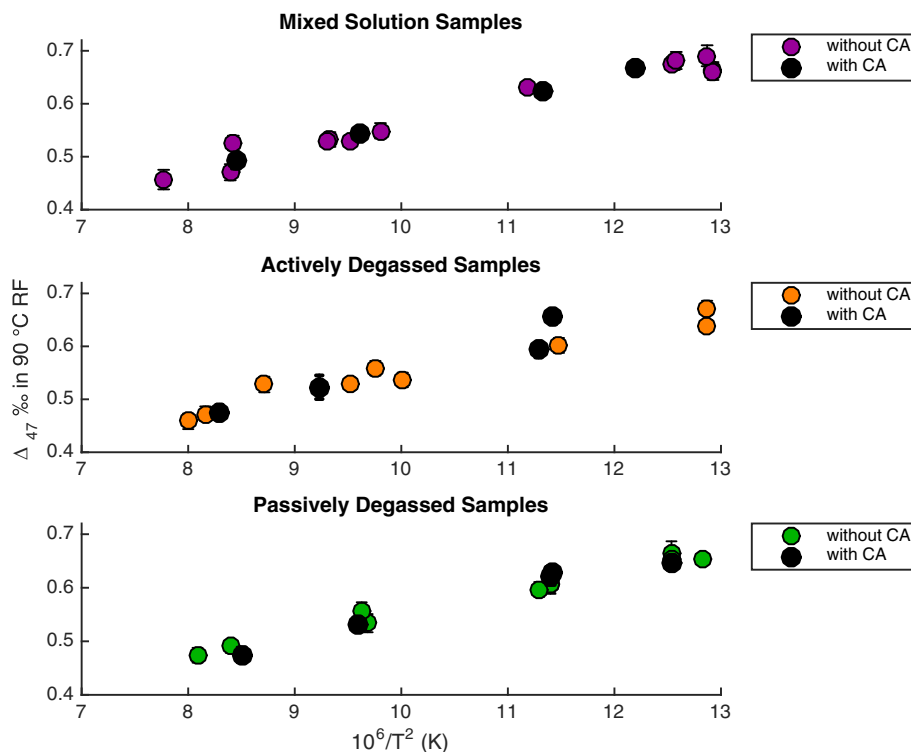


Fig. 1. Synthetic carbonate samples grown with carbonic anhydrase (black) and without (color). Δ_{47} (‰) plotted against growth temperature. Error bars are 1 SE, and are generally smaller than the symbol. (For interpretation of the references to colour in this figure legend, the reader is referred to the web version of this article.)

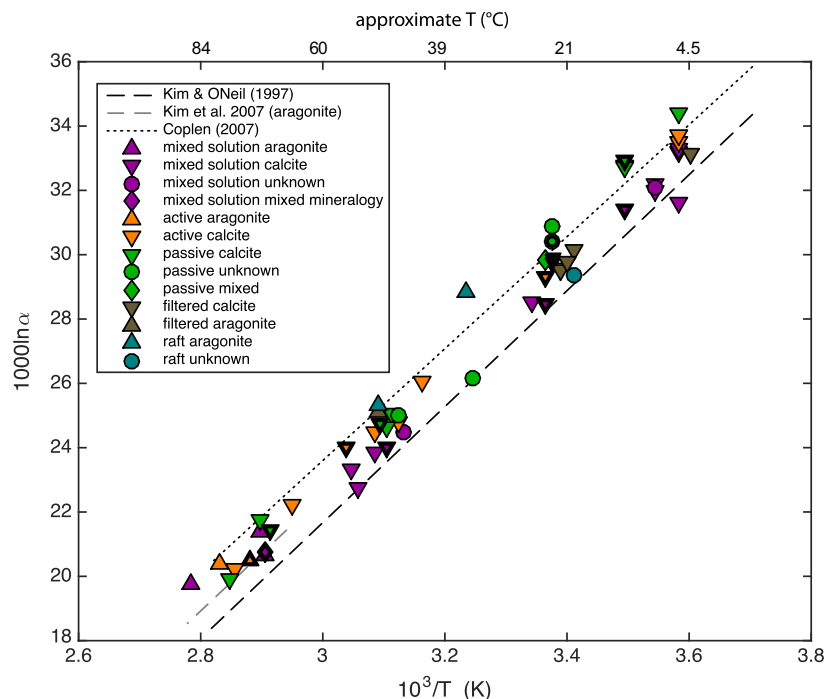


Fig. 2. Mineral-water fractionation in oxygen isotopes plotted versus carbonate growth temperature. Error bars are smaller than marker size. Colors indicate precipitation method and shape indicates mineralogy. Samples with bold outline were grown in the presence of CA ($n = 13$). Our samples mostly fall between the [Kim and O'Neil \(1997\)](#) relationship measured in synthetic carbonates and the [Coplen \(2007\)](#) relationship measured from Devils Hole calcite, and they fall within the range expected for carbonates grown at laboratory growth rates ([Watkins et al., 2014](#)). (For interpretation of the references to colour in this figure legend, the reader is referred to the web version of this article.)

all of the different precipitation methods are averaged, the standard deviations of those averages range from 0.010 to 0.024‰. For comparison, these values are better than or as good as the reproducibility of individual replicates of our in-house calcite standards during the same time period as the samples (C64: standard deviation (SD) $\Delta_{47} = 0.023\text{‰}$; Coral: SD $\Delta_{47} = 0.025\text{‰}$). This suggests that the spread of measured Δ_{47} values reflects the expected analytical variability.

Because all sample types yield Δ_{47} results that are indistinguishable within measurement error, we combine the 56 samples to produce a linear relationship that can be used as a calibration for samples reacted at 90 °C with growth temperatures approximately between 4 and 85 °C ([Table 2](#)):

$$\Delta_{47} = 0.0417 \pm 0.0013 \times 10^6 / T^2 + 0.139 \pm 0.014 \quad (1)$$

The mean AFF calculated for the 11 samples reacted at both 25 and 90 °C is $0.098 \pm 0.025\text{‰}$ (error is propagated from the SE of replicates of samples). This estimate overlaps with previous estimates ([Guo et al., 2009](#); [Passey et al., 2010](#); [Henkes et al., 2013](#); [Wacker et al., 2013](#); [Defliese et al., 2015](#)). The same trends in Δ_{47} vs. temperature persist for the different sample types when reacted at 25 °C, and the measurements made after 25 °C and 90 °C reaction are within error of each other when projected into the 25 °C reference frame ([Fig. 3](#)). The choice of AFF does not change this result. Although the 25 °C acid digestion

data are sparse, all of the Δ_{47} – temperature regressions are similar to those observed for the data produced using 90 °C acid digestion ([Table 2](#)).

4. DISCUSSION

Our results shed light on several aspects of carbonate precipitation that have been proposed to affect $\delta^{18}\text{O}$ and Δ_{47} , including the results of (1) experiments replicating previous studies while providing ancillary information that is not typically reported (e.g., pH), (2) new experiments isolating variables that differed among previous studies and using CA to promote DIC equilibration. At first, we hold analytical methods constant, and then we change acid digestion temperature, and use the [Brand et al. \(2010\)](#) ^{17}O correction parameters.

4.1. Insights into carbonate precipitation variables that do not influence measured Δ_{47}

Previous workers have suggested that carbonate Δ_{47} -temperature calibrations diverge because of disequilibrium carbonate precipitation (e.g. [Dennis and Schrag, 2010](#); [Dennis et al., 2011](#); [Henkes et al., 2013](#); [Zaarur et al., 2013](#); [Fernandez et al., 2014](#); [Tang et al., 2014](#)). Indeed, isotopic equilibrium is unlikely to be achieved in laboratory experiments ([Watkins et al., 2014](#)), and

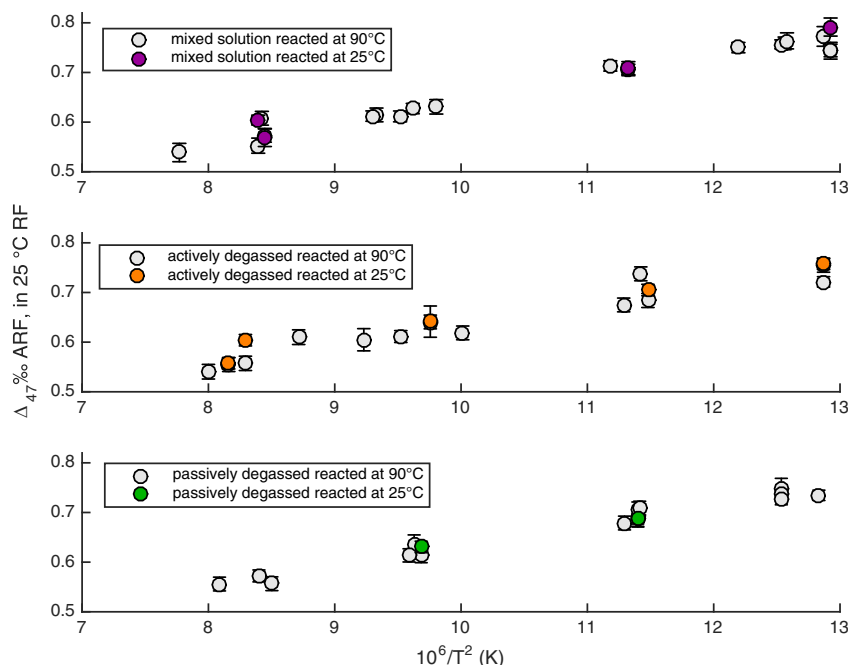


Fig. 3. Δ_{47} values for samples digested in 25 and 90 °C phosphoric acid plotted against growth temperature. Error bars are 1 SE. The measured Δ_{47} value for samples after digestion at 25 °C is within error of the measured Δ_{47} value after digestion at 90 °C (samples reacted at 90 °C are corrected with the AFF of 0.082‰ from Defliese et al. (2015)) (Table A2).

can occur among the DIC species in solution, at the solution-air boundary layer, or between solution and the mineral surface (Zeebe, 1999, 2007; Fenter and Sturchio, 2004, 2012; Geissbühler et al., 2004; Affek, 2013; Fenter et al., 2013; Affek and Zaarur, 2014; Tripathi et al., 2015). Several of our observations eliminate specific precipitation methods as the cause of calibration discrepancies by showing that these methods do not cause divergences in measured Δ_{47} .

First, our observation that the use of CA in solution does not measurably influence $\delta^{18}\text{O}$ or Δ_{47} values of calcium carbonates grown in this study (Fig. 1, Fig. 2) suggests that disequilibrium in the DIC pool does not exist, or is not large enough to cause measurable isotope effects in the precipitate material of this work or in those of the previous work whose methods we replicated. DIC species take about 5 hours to equilibrate at 25 °C and a pH of 7 (Zeebe, 1999; Wang et al., 2009; Uchikawa and Zeebe, 2012). For many of our room temperature samples, we first observed precipitate material in approximately that amount of time, so it seems possible that the calcium carbonate could inherit some of the original isotopic composition of the NaHCO_3 and CaCO_3 from DIC species that are not fully equilibrated (e.g., Henkes et al., 2013). We speculate that we do not observe a change in $\delta^{18}\text{O}$ or Δ_{47} values when we add CA because only a small fraction of all calcite precipitated during the early periods when water-DIC disequilibrium may occur.

DIC disequilibrium also may be caused by rapid CO_2 degassing, but our results suggest that the precipitation methods used in previous studies and replicated here do

not inherently cause dissimilar Δ_{47} values through this mechanism. It has been suggested that actively degassing solution could cause faster degassing rates, faster precipitation rates, and thus kinetic isotope effects (Fernandez et al., 2014). In contrast, it has also been suggested that the open-atmosphere passive degassing method causes disequilibrium because the carbonate represents a mix of surface and bulk solution conditions (Affek and Zaarur, 2014). Our experiments are the first to vary active vs. passive degassing under a constant analytical setting. The passively and actively degassed samples, for which the only difference is N_2 bubbling, have Δ_{47} values that are statistically indistinguishable for a given precipitation temperature (Fig. 4). The mixed solution samples, which do not have N_2 or CO_2 bubbling, are within measurement error of the other sample types. Our ability to resolve disequilibrium effects is limited by the SE of the individual samples and the SE of the calibration equations. Nevertheless, agreement within 1 SE of our samples that replicate previously published precipitation methods indicates that disequilibrium due to CO_2 degassing is unlikely to explain the calibration slope discrepancies. Taken together, observations from our CA experiments and N_2 bubbling comparisons support the idea that disequilibrium among DIC species in solution is less important than the kinetics of transporting, attaching, and detaching DIC species at the mineral surface in causing Δ_{47} disequilibrium when it occurs (Affek and Zaarur, 2014; Watkins and Hunt, 2015).

While our findings suggest that DIC disequilibrium and CO_2 degassing are not the cause of calibration discrepancies in previous studies, we note isotope effects due to rapid CO_2

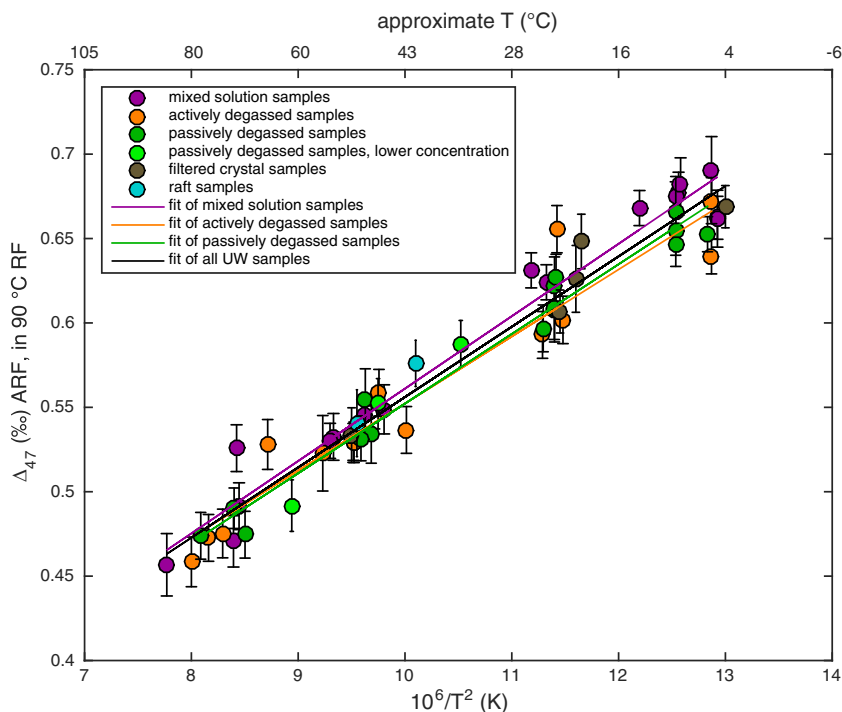


Fig. 4. Δ_{47} vs. growth temperature for all synthetic carbonate samples from this work. Error bars are 1 SE. The black regression is the regression through all UW samples processed with Brand et al. (2010) values (Eq. (1)).

degassing have been observed in other samples. Rapid CO_2 degassing has been shown to cause a decrease in Δ_{47} values and an increase in $\delta^{13}\text{C}$ and $\delta^{18}\text{O}$ values in some natural inorganic calcites like speleothems (Mickler et al., 2004; Daëron et al., 2011; Kluge and Affek, 2012; Kluge et al., 2013; Affek et al., 2014), as well as in synthetic calcium carbonates precipitated in the bulk solution (Guo, 2009) and as rafts at the water-surface interface (Affek and Zaarur, 2014). We therefore expected the raft carbonates of this study to have Δ_{47} values that differed from the other sample types because they grew at the solution surface, presumably during rapid CO_2 degassing (Affek and Zaarur, 2014). However, the raft Δ_{47} values were not different from the other samples grown in bulk solution (i.e., samples that had to be scraped off the bottom of the flask) (Fig. 4). Watkins and Hunt (2015) predict that kinetic effects in Δ_{47} can be as small as 0.01‰, which is within our measurement uncertainty. Therefore, it is possible that these raft carbonates experienced Δ_{47} disequilibrium that cannot be resolved with current analytical precision. It also may be possible that, despite their floating raft morphology, these samples were not formed due to rapid CO_2 degassing at the surface boundary layer, although we are not aware of a process that forms floating carbonates other than rapid degassing at the surface. Finally, we note that the raft carbonates precipitated in this study and those of Affek and Zaarur (2014) were produced by similar, but not identical methods. The two raft carbonates formed in the present study were unintentionally produced from solutions that were (gently) stirred with N_2 bubbles, while the 14 raft cal-

cites of Affek and Zaarur (2014) were precipitated from solutions that were not stirred at all; stirring can change the thickness of the surface boundary layer. Nevertheless, our observations raise the possibility that the large kinetic effects observed by Guo (2009) and Affek and Zaarur (2014) are not inherent to all carbonate materials formed floating at the solution-air interface in synthetic carbonate experiments.

Recent work raises the possibility that solution pH, ionic concentration and carbonate growth rate could contribute to differences among previous calibrations (e.g., Affek and Zaarur, 2014; Hill et al., 2014; Tang et al., 2014; Watkins and Hunt, 2015; Tripathi et al., 2015). To the extent possible, our experiments provide insight into the effects of these variables on Δ_{47} in previous calibration studies whose experiments we replicated, and by isolating the effect of ionic concentration in new experiments.

Our findings are consistent with theoretical predictions that the pH effect on Δ_{47} is likely too small to be resolved in carbonate precipitated from solutions in the pH range we investigated, and suggest that previous calibration studies were likely conducted in the same pH range (Hill et al., 2014; Tripathi et al., 2015; Watkins and Hunt, 2015). Most previous carbonate Δ_{47} -temperature calibration studies do not report pH. However, the pH values we report here likely represent the pH range of previous calibration studies whose methods we replicated. pH in calibration samples could vary systematically with carbonate growth temperature because CO_2 solubility depends on temperature; therefore variability in pH could affect Δ_{47} -temperature

sensitivity. pH can influence Δ_{47} values of carbonate by changing DIC speciation. HCO_3^- dominates at $\text{pH} \sim 5$ – 10 , and CO_3^{2-} dominates at higher pH values (depends on temperature and salinity; Hill et al., 2014; Tripathi et al., 2015). CO_3^{2-} has a lower Δ_{47} than HCO_3^- , so calcium carbonate minerals precipitated at high pH are expected to have lower Δ_{47} (Hill et al., 2014; Tripathi et al., 2015). Our samples are within the pH range where HCO_3^- is dominant (range of 5.67–8.77). The calculations of Watkins and Hunt (2015) suggest that in this pH range, Δ_{47} is expected to vary by $<0.01\%$ at typical experimental growth rates. Consistent with these predictions, we observe no measurable pH effect on Δ_{47} values (Hill et al., 2014; Tang et al., 2014; Watkins and Hunt, 2015). These observations indicate pH should not have a significant influence on measured Δ_{47} in our experiments—or on previous <100 °C calibrations, which are likely within the same pH range.

Our results are consistent with previous empirical studies that have shown that growth rate does not measurably influence Δ_{47} within the range of experimental growth rates (Tang et al., 2014; Kele et al., 2015). A process-based isotope model suggests that growth rate may influence Δ_{47} values, but not by a measurable amount in a pH range of 7–9 (Watkins and Hunt, 2015). We lack measurements of growth rate for each sample (apart from knowing total mass collected and experiment run time). Qualitatively, we observe that the mixed solution and filtered crystal sample types grow, on average, more slowly than the actively and passively degassed sample types at a given temperature. These limited observations combined with our finding that the Δ_{47} values agree among all sample types support previous work suggesting that growth rate within the range observed in laboratory experiments does not influence Δ_{47} .

Our experiments also suggest that ionic strength and stoichiometric proportions are not likely responsible for previous calibration discrepancies. Stoichiometric excess of Ca^{2+} could enhance kinetic isotope fractionations at the mineral surface (suggested by Affek and Zaarur, 2014). We precipitate samples that start with both balanced stoichiometry and unbalanced stoichiometry (excess of Ca^{2+}), and in a range of salt concentrations of 7–20 mM (Table A2). The samples grown with lower ionic concentration and unbalanced-stoichiometry have Δ_{47} values that are within measurement error of the other samples grown with a higher ionic concentration and stoichiometric balance (Fig. 4, Table A1). The ionic strength and unbalanced stoichiometry likely does not influence Δ_{47} in our samples, or in those of previous calibrations whose methods we replicated, perhaps because Δ_{47} is not sensitive to growth rate within the range observed in laboratory experiments (Tang et al., 2014; Affek and Zaarur, 2014; Watkins and Hunt, 2015).

In summary, our approach of analyzing synthetic carbonates in a single laboratory circumvents many complications that make it difficult to directly compare the results of previous studies—enabling us to rule out calcium carbonate precipitation method as the cause of calibration discrepancies. It is difficult to envision an untested sample preparation method that might disproportionately affect samples with high Δ_{47} values to change the calibration slope. How-

ever, future calcite precipitation experiments that more closely monitor pH throughout the experiment, and quantify growth rate of carbonates and solution degassing rate could shed light on some of the variability that is observed in calibration samples.

4.2. $\delta^{18}\text{O}$ Fractionation between synthetic calcium carbonates and water

The calcite-water oxygen isotope fractionation factors calculated for all samples can be compared to previous predictions. True oxygen isotope equilibrium that is likely exemplified by the slow-growing Devils Hole calcite (Coplen, 2007) is unachievable for calcites grown at laboratory growth rates (Watkins et al., 2014). Our samples fall approximately within the range of expected fractionation factors for samples grown at laboratory growth rates (Watkins et al., 2014), which is also near the values of Kim and O'Neil (1997) (Fig. 2). The spread among our samples is likely due to small variations in solution pH and growth rate (Watkins et al., 2014); precision for $\delta^{18}\text{O}$ measurements allows better resolution of these effects where the precision for Δ_{47} does not currently allow for observation of these effects. The spread we observe is comparable to that observed in calcite-water fractionation in the studies of Zaarur et al. (2013), Affek and Zaarur (2014), and Dennis and Schrag (2010). For our samples, deviation from the Kim and O'Neil (1997) relationship does not correlate with deviation from Δ_{47} predictions (the choice of Δ_{47} calibration or theoretical curve from which to measure Δ_{47} deviation does not matter). This suggests that Δ_{47} is not measurably influenced by the small changes in pH and growth rate that influence $\delta^{18}\text{O}$ fractionation. Because the samples in this study plot near previous $\delta^{18}\text{O}$ carbonate-water predictions, they likely precipitated from a DIC pool that was isotopically equilibrated, even if there was no solution storage time. This hypothesis is further supported by agreement between our samples grown with or without CA.

4.3. Acid digestion temperature does not change Δ_{47} -temperature sensitivity

Our observation that the Δ_{47} values of samples reacted in 25 and 90 °C acid show the same Δ_{47} -temperature sensitivity confirms that acid temperature is not responsible for slope discrepancies (Fig. 3, Deffiesse et al., 2015). Historically, laboratories that reacted samples offline in individual acid vessels at 25 °C mostly display a steeper Δ_{47} -temperature calibration slope (e.g., Ghosh et al., 2006; Zaarur et al., 2013) compared to laboratories that react samples at 90 °C in a common acid bath (e.g., Dennis and Schrag, 2010; Wacker et al., 2014). However, exceptions to this pattern further show that acid digestion temperature is not a simple explanation for calibration discrepancies. For example, Tripathi et al. (2015) reacted samples at 90 °C but report a slope that is within error of the slope of Zaarur et al. (2013), who reacted at 25 °C (Table 2; Tripathi et al. (2015) calibration that includes all samples). Also, Petrizzo et al. (2014) reacted at 25 °C, but report a slope of 0.0358 ± 0.0060 , which is within error of

the slope of [Dennis and Schrag \(2010\)](#). This pattern could potentially be explained by the observation that reacting small (<5 mg samples) in a vessel at 25 °C can produce higher Δ_{47} values ([Wacker et al., 2013](#)).

All of the samples in our study were reacted in 6–9 mg aliquots avoiding such potential complications, but grain size did vary among the samples. It is conceivable that AFF could depend on grain size because smaller grains could more easily equilibrate with water present in the phosphoric acid (similar to the small grain size re-equilibration observed in the Kiel devices by [Tobin et al., 2011](#)). If this effect was significant and grain size was correlated with precipitation temperature, using a constant AFF to project samples in the 25 °C reference frame would produce slope inaccuracies. However, the AFF that we measure does not appear to depend on calcium carbonate grain size. A linear regression between grain size and AFF has an r^2 of 0.01, $p = 0.79$; other types of regressions (logarithmic, polynomial, etc.) do not yield better fits. This observation suggests that grain size and texture may not influence AFF, but a more thorough investigation should be undertaken given that we tested a small range of grain sizes and reacted a relatively small number ($n = 11$; 2 to 4 replicates each) of samples at both 25 and 90 °C.

4.4. Comparison to previously published Δ_{47} –temperature calibrations processed using [Santrock et al. \(1985\)](#) parameters

We compare our samples to previously published calibration data, taking into account the effects of ^{17}O correction parameters on Δ_{47} values to the extent possible. To our knowledge, previously published carbonate clumped isotope calibration studies processed data using the traditional [Santrock et al. \(1985\)](#) parameters to correct for ^{17}O interference in $\delta^{13}\text{C}$ measurements by mass spectrometry (e.g., [Affek and Eiler, 2006](#); [Huntington et al., 2009](#)). Visual inspection of our samples re-calculated with the traditional [Santrock et al. \(1985\)](#) parameters plotted with calibration samples from previous work highlights the spread in measured Δ_{47} for a given temperature (up to 0.1‰) ([Fig. 5](#)) (values in [Table A3](#)). None of our samples are able to replicate the high Δ_{47} values at lower temperatures reported by [Ghosh et al. \(2006\)](#), even by precipitating samples using almost identical methods (dissolve and filter CaCO_3 , actively degas CO_2 with N_2) ([Fig. 5](#), [Table 2](#)). [Kluge et al. \(2015\)](#) also uses very similar precipitation methods, but do not produce calibration slopes that are as steep as the [Zaarur et al. \(2013\)](#) calibration. Together, these

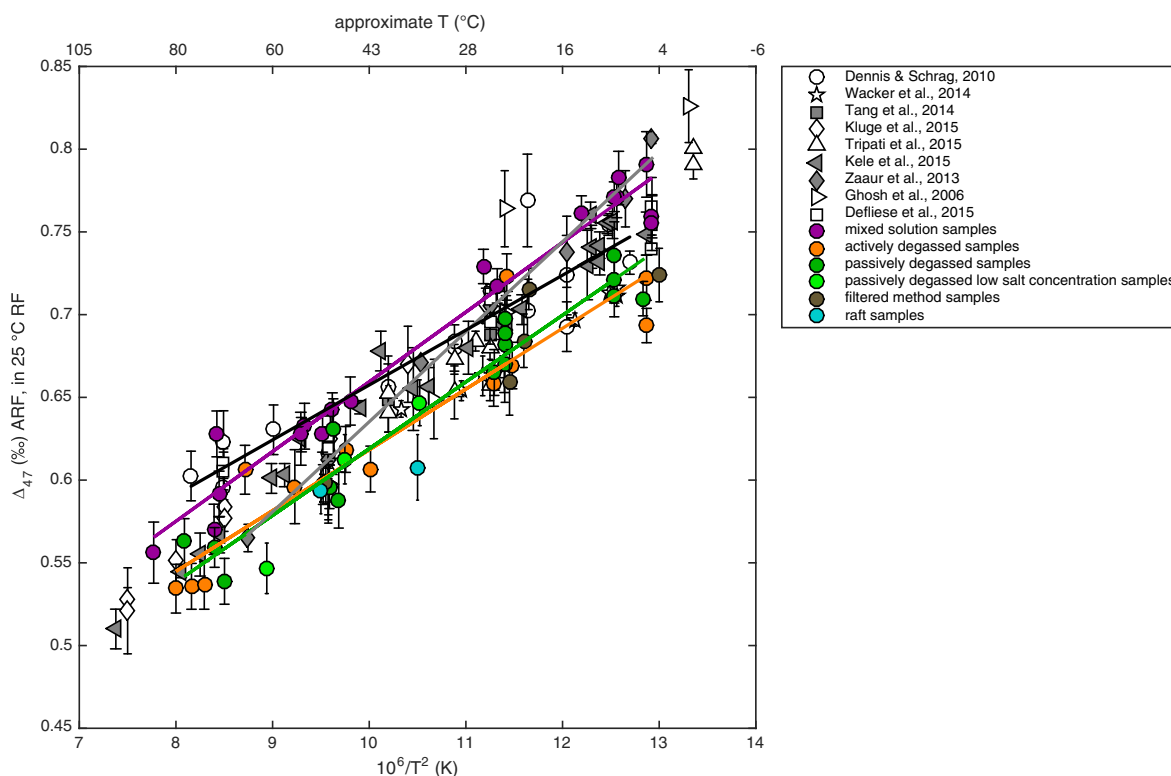


Fig. 5. Δ_{47} vs. growth temperature for synthetic carbonate samples from this work, and previous synthetic and abiogenic calibration samples. Colored samples and linear regressions are from this work. The solid gray line is the [Zaarur et al. \(2013\)](#) calibration and the solid black line is the [Dennis and Schrag \(2010\)](#) calibration. In order to compare our samples with those from previous work, the Δ_{47} values of our carbonate samples in this figure have been calculated using ^{17}O correction values of [Santrock et al. \(1985\)](#) ([Schauer et al., 2016](#)).

observations may suggest that precipitation method is not responsible for the relatively high Δ_{47} observed by Ghosh et al. (2006) at low temperatures, consistent with the results of our study. However, these comparisons are inherently flawed because they rely on Δ_{47} data that may be inaccurate to some degree due to the choice of ^{17}O correction parameters.

4.5. The influence of ^{17}O correction parameters on measured Δ_{47} values and comparison to calibration data processed using Brand et al. (2010) parameters

Having ruled out precipitation method and acid digestion method as likely causes of calibration discrepancies, we discuss the potential implications for calibration data of the recent finding that the choice of ^{17}O abundance corrections used to calculate Δ_{47} influences the accuracy of sample and absolute reference frame data (Daëron et al., 2016; Olack and Colman, 2016; Schauer et al., 2016). If the Santrock et al. (1985) ^{17}O correction values are used and the $\delta^{13}\text{C}$ composition of the reference frame gases, mass spectrometer working gas and/or sample gas differ, inaccuracies in calculated Δ_{47} values emerge (Daëron et al., 2016; Schauer et al., 2016). Thus differences in the isotopic compositions of synthetic carbonates, the mass spectrometer working gas, and/or the equilibrated gases used to construct the absolute reference frame could compromise the validity of inter-laboratory comparisons. Using the parameters recommended by Brand et al. (2010) to correct for ^{17}O abundance in CO_2 has been shown to minimize these inaccuracies (Daëron et al., 2016; Olack and Colman, 2016; Schauer et al., 2016).

Our dataset highlights the potential for the choice of ^{17}O correction parameters to influence calibration accuracy and agreement. In this study we present data processed using the parameters recommended by Brand et al. (2010) (Fig. 4). Schauer et al. (2016) show that re-processing our data using the Santrock et al. (1985) values traditionally used in clumped isotope studies causes up to 0.06‰ bias in some of our sample Δ_{47} values, and results in a large and spurious apparent disagreement between the mixed solution and other sample Δ_{47} data (Figs. 5 and 6a, Table A3; see Schauer et al., 2016, for details). It is not straightforward to predict how re-processing previously published data using the Brand et al. (2010) values will influence calibration samples from different laboratories; the magnitude and direction of change likely depend on the bulk composition of the absolute reference frame gases, the working gas, and the sample gas (Daëron et al., 2016). However, examination of our data provides strong evidence that other calibration samples could be affected significantly.

We also present the chicken eggshell as a biogenic data point available that has been processed with both Santrock et al. (1985) and Brand et al. (2010) ^{17}O parameters (Fig. 6). The egg displays closer agreement with the UW synthetic calibration samples when processed with the Brand et al. (2010) parameters (Fig. 6). In contrast, Eagle et al. (2015) suggest that their eggshell calibration

agrees well with the Ghosh et al. (2006) synthetic calibration as published originally (presumably with the Santrock et al. (1985) values). It remains to be determined if this agreement will hold when/if both calibrations are reprocessed with Brand values. Without further analysis, it seems that the choice in ^{17}O corrections is not the only variable that controls agreement between synthetic and biogenic data. Our single data point (the egg) does not allow for a comprehensive discussion of how biogenic data and their agreement with synthetic calibrations may be affected by the choice of ^{17}O parameters, but we hope that it may be a helpful reference for future workers.

A handful of synthetic carbonate data have been calculated using the Brand et al. (2010) ^{17}O correction factors, and can be directly compared with our data (Fig. 6) to demonstrate how the choice of ^{17}O parameters influences calibration data. Daëron et al. (2016) recalculate the Δ_{47} values of 5 of the 7 synthetic carbonate samples analyzed at Yale University by Zaarur et al. (2013) and 5 previously unpublished synthetic carbonates analyzed at LSCE (University of Paris-Saclay) using the Brand et al. (2010) parameters. Daëron et al. (2016) show that the slopes of the LSCE and Yale calibrations are not affected by the choice of ^{17}O parameters, but that the intercepts move further apart when reprocessed with the Brand et al. (2010) values. Similarly, the slope of our calibration is not affected by using the Brand et al. (2010) parameters. In contrast with Daëron et al. (2016), the dispersion of intercepts in our dataset is reduced (Figs. 4 and 6, Eq. (1); Schauer et al., 2016). These observations suggest that inaccuracies due to the choice ^{17}O correction parameter may explain some of the large dispersion among previous calibration data, but they likely do not explain the large slope discrepancies in previous clumped isotope calibrations.

However, we suggest the approach of focusing on slopes to compare calibration data may be inappropriate because regression slopes are easily influenced by aliasing due to small sample population size. The calibration comparison in Fig. 6b and the large population size of our dataset make it possible to evaluate this issue quantitatively. For example, when we repeat 10,000 times the exercise of randomly selecting 5 of our 56 calibration samples and fitting a line through them, 11% of the resampled populations produce a slope that is within error of the Yale calibration slope (0.055 ± 0.007), and 54% of the resampled populations produce a slope that is within error of the LSCE calibration slope (0.0388 ± 0.0046). Results are similar when the exercise is performed with a randomly selected sample size of 13, which is the number of samples used in the Dennis and Schrag (2010) calibration. Future workers who wish to differentiate between calibration lines should employ statistical tests that consider the sample population size. Instead of differentiating between calibrations, we believe that the calibration equation that is most robust to outliers and small population sizes is one that considers all available calibration sample data generated in different laboratories using comparable data processing methods. We present a

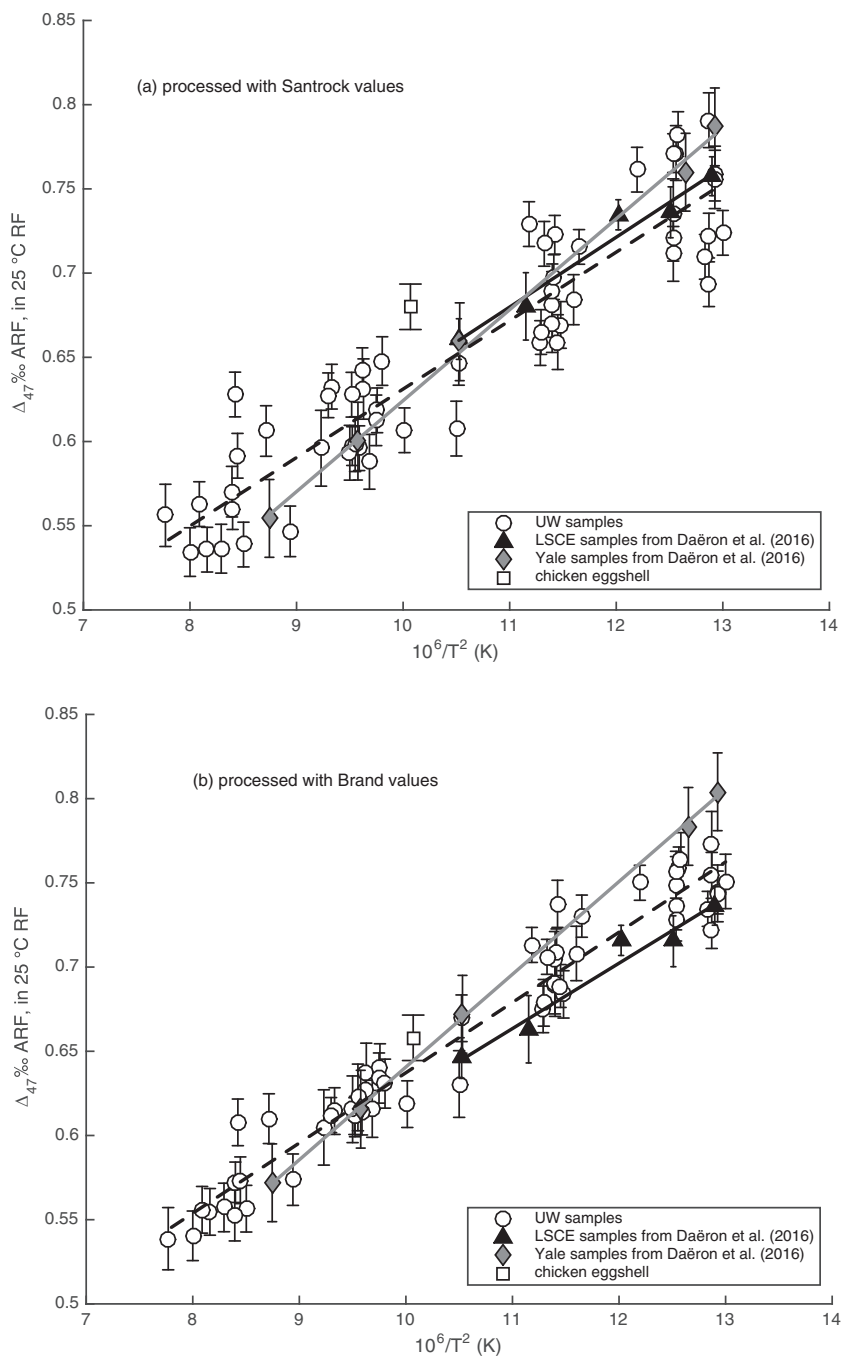


Fig. 6. Δ_{47} vs. growth temperature for synthetic carbonate samples from this work, and from LSCE and Yale as presented in the supplementary material in Daëron et al. (2016). Values are presented in the 25 °C reference frame (UW and LSCE samples reacted at 90 °C are corrected with the AFF of 0.082‰ from Defiense et al. (2015)). The solid gray line is the fit to the Zaarur et al. (2013) samples, the dashed black line is the fit to the UW samples, and the solid black line is the fit to the Paris samples. A) Samples processed using the Santrock et al. (1985) ^{17}O correction parameters. B) Samples processed using the Brand et al. (2010) ^{17}O correction parameters.

calibration equation that combines our samples with those from LSCE and Yale processed with Brand et al. (2010) in the 25 °C reference frame ($n = 66$, $r^2 = 0.942$):

$$\Delta_{47} = 0.0422 \pm 0.0013 \times 10^6/T^2 + 0.215 \pm 0.014 \quad (2)$$

We note that a source of unquantifiable error in this equation is the choice of AFF; here we use 0.082‰ (Defiense et al., 2015) to correct the UW and LSCE data, but recognize that this AFF may change when/if it is recalculated with the Brand et al. (2010) parameters. We offer

the above equation with the caveat that a community effort to reprocess all calibration and AFF samples with the [Brand et al. \(2010\)](#) parameters and/or produce new calibration data that can be compared in the same framework will result in a more accurate calibration equation. We advocate that this effort is the most promising approach for arriving at a calibration that is universal to all laboratories.

4.6. Additional possible analytical and data-processing controls on Δ_{47} disagreements

While we think that using appropriate ^{17}O correction parameters may significantly improve inter-laboratory agreement, we discuss other differences in analysis techniques that could potentially change measured Δ_{47} values that merit systematic evaluation. These analytical differences may not directly influence calibration slopes, but they may have with implications for dispersion in calibration data.

First, the precise density of the phosphoric acid used could influence oxygen exchange during carbonate dissolution, and is not currently well documented ([Colman and Olack, 2015](#); [Defliese et al., 2015](#)). Similarly, the distance from the acid bath to the water traps on preparation lines could contribute to CO_2 gas re-equilibration with water (as observed in acid vessels in [Wacker et al., 2013](#)). Also, methods used to remove contaminants vary or are not used (e.g., the use of gas chromatograph or packed columns, with or without He carrier gas, operating at different temperatures; [Ghosh et al., 2006](#); [Dennis and Schrag, 2010](#); [Bernasconi et al., 2013](#); [Petersen et al., 2016](#)). Laboratories that use a gas chromatography (GC) column report similar calibrations (e.g., [Zaarur et al., 2013](#); [Tripathi et al., 2015](#) (all samples)), whereas laboratories that use a vacuum line Porpak Q trap report similar calibrations (e.g., this work; [Dennis and Schrag, 2010](#); [Kluge et al., 2015](#)). Laboratories also vary the method of storing or transferring purified CO_2 to the mass spectrometer for analysis (e.g., using a break seal or not). Additionally, there may be artifacts that arise from differences in the way laboratories measure backgrounds (i.e., backgrounds measured with or without gas flowing into the mass spectrometer source; [He et al., 2012](#); [Bernasconi et al., 2013](#); [Fiebig et al., 2015](#)) that remain to be explored systematically. The influence of these analytical differences on measured Δ_{47} values remains to be explored systematically.

4.7. Implications for isotope effects in natural abiogenic carbonates

Our unique dataset shows consistent Δ_{47} values for calcium carbonates synthesized with diverse precipitation conditions, suggesting that natural abiogenic calcium carbonates preserved in geologic archives should also reliably record temperature over a variety of precipitation conditions. Reliable carbonate geothermometers can be found in environments that host solutions where HCO_3^- is the dominant DIC species ($\sim\text{pH}$ 5 to 10, such as soil waters). Small changes in solution chemistry in these environments

will still result in Δ_{47} values that can be directly compared to abiogenic laboratory precipitation experiments ([Tripathi et al., 2015](#)). Critically, we also show that carbonates produced in solutions that are not necessarily in DIC equilibrium (all of our experiments that do not have CA) have isotopic compositions that are indistinguishable from samples produced in known DIC equilibrium (all of our experiments that do have CA). This observation indicates that small changes in the source DIC pool should not significantly influence the isotopic compositions of natural samples. Disequilibrium Δ_{47} values, when observed, instead likely result from cases where DIC species are far from equilibrium, or from kinetic processes at the solution-mineral interface ([Kluge et al., 2014](#); [Tripathi et al., 2015](#)), although the magnitude, and even direction, of such effects remain highly uncertain ([Watkins and Hunt, 2015](#)).

Our samples may offer insight into the effect of CO_2 degassing on natural samples. Despite degassing CO_2 with different methods, our Δ_{47} results are consistent. We do not reproduce large kinetic effects that might be expected from degassing, even in our raft-morphology carbonates (e.g., as observed in the raft carbonates of [Affek and Zaarur, 2014](#)). This may suggest that Δ_{47} equilibrium of other natural samples is likely unaffected by degassing unless the carbonates are precipitated in solutions that have high concentrations of CO_2 compared to ambient air, or where the water–air interface is large compared to the reservoir, such as in speleothems (e.g., [Daëron et al., 2011](#); [Kluge and Affek, 2012](#)).

Our carbonate synthesis experiments are most similar to the formation processes of natural samples such as travertines, tufas, and vein, soil and lake carbonates. Vent and open-air pool travertines/tufas precipitate during the initial degassing of a small fraction of the CO_2 dissolved in solution, and thus are similar to our samples in that they do not experience measurable kinetic effects due to degassing ([Kele et al., 2015](#)). Similarly, pedogenic carbonates typically grow in soil waters that are slowly degassed and become supersaturated during drying events, and are thought to precipitate in near-equilibrium conditions (e.g., [Quade et al., 2007, 2013](#); [Breecker et al., 2009](#); [Burgener et al., 2016](#)). Our calibration samples are also analogous to open lake carbonates that form in response to degassing caused by biotic removal of CO_2 ([Hren and Sheldon, 2012](#)). In contrast, carbonates grown in closed, evaporative lakes may grow under a relatively higher degree of supersaturation and pH ([Reddy, 1995](#)), which could invalidate the comparison with our calibration samples. Similarly, alkaline spring carbonates may have isotope values that are influenced by hydroxylation of CO_2 and other kinetic effects ([Falk et al., 2016](#)). We suggest through these comparisons that our samples likely represent processes relevant to natural, inorganic samples grown in physiochemical conditions that can be found in a variety of geologic settings. As such, we anticipate that the calibration we present in Eq. (1) can be used to estimate the growth temperature of a wide variety of natural carbonates even when their precipitation pathway is highly variable.

5. CONCLUSIONS

Several suites of calcites, grown using various precipitation methods and acid digestion temperatures, while holding other analytical methods constant, suggest a constant Δ_{47} -temperature relationship. Our findings corroborate previous work showing that changing the temperature of acid digestion does not change the temperature sensitivity of the Δ_{47} -temperature relationship. We further suggest that calibration discrepancies are not a direct result of the precipitation methods used by previous workers; these methods do not appear to cause measurable Δ_{47} differences due to disequilibrium in the DIC species or CO_2 degassing method.

Our observations suggest that natural samples grown in moderate pH (5–10) and near-equilibrium conditions between 4 and 85 °C can be represented by a calibration that includes the synthetic samples from this work (Eq. (1), Table 2). The similarity of isotopic compositions among our samples even with diverse precipitation methods suggests that many natural carbonates can be used as dependable geothermometers. The large number of data points ($n = 56$ samples) makes this calibration robust to outliers, and illustrates that the approach of using slopes to compare calibration regressions is vulnerable to aliasing. However, the dispersion of some calibration data exceeds that which can be explained by analytical error and acid fractionation uncertainties. This work highlights the need for systematic study of how CO_2 gas purification, acid preparation, background corrections, and most importantly ^{17}O correction parameters assumed during Δ_{47} calculations could influence measured Δ_{47} values.

ACKNOWLEDGEMENTS

We thank Associate Editor Hagit Affek for her invaluable conversations and reviews that greatly improved our discussion of kinetics and the implications of our work to clumped isotope calibrations. We also thank Jens Fiebig and two anonymous reviewers for their comments that improved this manuscript. This material is based on work supported by the National Science Foundation Graduate Research Fellowship Program under Grant No. DGE-1256082 to JRK. We also gratefully acknowledge funding from the National Science Foundation under grants EAR-1156134 and EAR-0955309 to KWH and from the Geological Society of America under a Graduate Student Research Grant to JRK. CS acknowledges support from the UW School of Oceanography. We thank Rebecca Smith, Adrienne Scott, and Paul Tosello for their assistance in the laboratory and with grain size analyses. We thank Scott Kuehner for assistance with microprobe imaging of our samples. We also acknowledge Tuesday Kuykendall and Tatyana Galenko (UW Materials Sciences and Engineering) for their assistance in acquiring and analyzing XRD data.

APPENDIX A

See Tables A1–A3.

APPENDIX B. SUPPLEMENTARY DATA

Supplementary data associated with this article can be found, in the online version, at <http://dx.doi.org/10.1016/j.gca.2016.10.010>.

Table A1
Experimental Conditions.

Sample	Precipitation Method	Average Growth Temperature (°C)	Standard Deviation of Temperature (°C)	Standard Deviation of Molarity	NaHCO_3 Molarity (mM)	$\text{CaCl}_2 \cdot \text{H}_2\text{O}$ Molarity (mM)	Molarity CA (if added, in μM)	Humidified N_2 ?	Growing Time (days)	Amount collected (grams)	Solution $\delta^{18}\text{O}$ (start, in permil vs SMOW)	Solution $\delta^{18}\text{O}$ (end in permil vs SMOW)	Solution pH (start)	Solution pH (end)	Solution Grain Size (d50, in μm)	Morphology
UWcp14_4C_2	Actively degassed	6	0.05	20	20	20		No	18	0.84	-10.38	-10.34	7.0	7.0		Calcite
UWcp14_4C_4	Actively degassed	6	0.05	20	20	20		Yes	41	0.8	-9.61	-10.31	6.38	5.85		Calcite
UWcp14_21C_1	Actively degassed	22	0.22	20	20	20		No	7	0.75	-10.62		6.75		3.1	Calcite
UWcp14_40C_1	Actively degassed	43	1.46	20	20	20		No	1	0.74	-10.86	-10.71	5.36	8.13	4.7	Calcite
UWcp14_50C_1	Actively degassed	47	0.36	20	20	20		No	7	0.7	-10.61	-10.54	7.62	8.19	4.7	Calcite
UWcp14_50C_2	Actively degassed	51	0.36	20	20	20		No	4	0.82	-10.61	-10.59	7.78	7.81		Calcite
UWcp14_60C_2	Actively degassed	66	2.31	20	20	20		No	2	0.80	-10.45	-10.4	6.70	7.08	4.2	Calcite

UWcp14_80C_1	Actively degassed	77	0.36	20	20		No	3	0.92	-10.38	-10.45	8.27	7.79	4.0	Calcite
UWcp14_80C_3	Actively degassed	80	0.64	20	20		No	4	0.93	-10.29	-10.22	6.65	7.82		Aragonite (97.6%), calcite (2.4%)
UWcp14_24C_CA_1	Actively degassed	24	0.76	20	20	25	No		0.25	-10.75	-10.78	7.70	7.58	3.7	Calcite
UWcp14_20C_CA_16	Actively degassed	23	0.42	20	20	24	Yes	6	0.75			6.00	7.01		Calcite
UWcp14_50C_CA_3	Actively degassed	56	0.63	20	20	25	No	4	0.74	-10.69	-10.68	7.42	8.12		
UWcp14_70C_CA_1	Actively degassed	74	0.95	20	20	25	No	2	0.88	-10.74	-10.58	7.54	8.16	7.0	Aragonite
UWcp14_4C_3	Passively degassed	6	0.05	20	20		No	42	0.82	-9.91	-10.40	6.57	6.61		Calcite
UWcp14_8C_2	Passively degassed	9	0.12	20	20		No	24	0.83	-10.28	-10.23	5.90			Calcite
UWcp14_8C_3	Passively degassed	9	0.12	20	20		No	17	0.80	-10.16	-10.32		6.56		Calcite
UWcp14_20C_9	Passively degassed	23	0.33	20	20		No	2	0.60	-10.51		6.71	7.24	3.6	Calcite
UWcp14_20C_4	Passively degassed	23	0.33	20	20		No	11	0.08	-10.69	-10.67	7.61			
UWcp14_20C_10	Passively degassed	24	0.43	20	20		No	4	0.43	-10.68	-10.62	6.67	7.77		Calcite (55.7%), vaterite (44.3%)
UWcp14_50C_5	Passively degassed	48	0.77	20	20		No	2	0.8	-10.51	-10.46	6.80	7.52	4.5	Calcite
UWcp14_50C_3	Passively degassed	49	0.12	20	20		No	1	0.67	-10.43	-10.55	6.98	7.01		Calcite
UWcp14_70C_4	Passively degassed	72	0.43	20	20		No	2	0.82	-10.54	-10.44	6.78	7.44	7.5	Calcite
UWcp14_80C_2	Passively degassed	78	1.28	20	20		No	1	0.72	-10.42	-10.39	6.61	7.28		Calcite
UWcp14_8C_CA_4	Passively degassed	9	0.12	20	20	19	Yes	34	0.87	-10.48	-10.44	5.71	7.07		Calcite
UWcp14_20C_CA_5	Passively degassed	23	0.33	20	20	25	No	11	0.05	-10.47	-10.49	7.48	7.62		
UWcp14_20C_CA_11	Passively degassed	23	0.34	20	20	25	No	7	0.49	-10.50	-10.46	6.81	8.08	9.0	Calcite
UWcp14_50C_CA_10	Passively degassed	50	0.74	20	20	25	No	4	0.8	-10.20	-10.18	6.15	6.80	3.9	Calcite (98%), aragonite (1.7%)

(continued on next page)

Table A1 (continued)

Sample	Precipitation Method	Average Growth Temperature (°C)	Standard Deviation of Temperature (°C)	NaHCO ₃ Molarity (mM)	Molarity CaCl ₂ ·H ₂ O (mM)	Molarity CA (if added, in μM)	Humidified N ₂ ?	Growing Time (days)	Amount collected (grams)	Solution δ ¹⁸ O (start, in permil vs SMOW)	Solution δ ¹⁸ O (end in permil vs SMOW)	Solution pH (start)	Solution pH (end)	Grain Size (d50, in μm)	Morphology
UWcp14_70C_CA_5	Passively degassed	70	0.89	20	20	25	No	3	0.86	-10.55	-10.46		7.91	5.9	Calcite
UWcp14_35C_1	Passively degassed	35	0.71	3.1	3.9		No	8	0.03	-10.63	-10.64	6.01	8.29		
UWcp14_50C_4	Passively degassed	47	1.32	3.2	4.0		No	8	0.05		-10.60	6.14	8.15		
UWcp14_60C_1	Passively degassed	61	0.86	3.0	3.9		No	6	0.08	-10.55	-10.45	6.15	8.08		Aragonite
UWcp14_3C_2	Mixed solution	9	1.67	3.1	3.9		No	88	0.04	-10.33	-10.18	8.77	7.09		
UWcp14_4C_1	Mixed solution	6	0.05	3.2	4.0		No	35	0.06	-10.20	-9.12		7.20		Calcite
UWcp14_4C_5	Mixed solution	6	0.05	3.1	4.0		Yes	42	0.05	-10.18	-10.04	6.80	7.16		Calcite
UWcp14_4C_6	Mixed solution	6	0.05	3.1	4.0		Yes	20	0.04			7.63	6.89		Calcite
UWcp14_8C_1	Mixed solution	9	0.12	3.1	4.0		No		0.05	-10.24	-10.19	7.94	6.78		Calcite
UWcp14_8C_6	Mixed solution	9	0.15	3.2	4.0		Yes	34	0.06			6.29	7.60		Calcite
UWcp14_20C_DS	Mixed solution	26	0.73	3.2	4.0		No	25	0.06	-10.37	-10.01	7.93	7.85	2.8	Calcite
UWcp14_50C_7	Mixed solution	54	1.98	3.2	4.0		No	4	0.04	-9.86	-10.30	8.54	8.26	6.2	Calcite (94.6%), aragonite (5.4%)
UWcp14_50C_8	Mixed solution	46	0.33	3.2	4.0		No	4	0.04	-10.37	-10.42	8.54	8.07		
UWcp14_50C_DS	Mixed solution	55	0.32	3.1	4.0		No	5	0.06	-10.26	-10.34	8.59	8.22		Calcite
UWcp14_50C_DS2	Mixed solution	51	0.3	3.1	4.0		No	17	0.07	-10.40	-10.19	8.56	8.51		Calcite
UWcp14_70C_DS2	Mixed solution	72	0.38	3.1	4.0		No	16	0.09	-10.35	-9.85	8.29	8.73	2.2	Aragonite
UWcp14_70C_2	Mixed solution	71	0.45	3.2	4.0		No	2	0.10	-10.43	-9.26	8.50	8.28		Aragonite
UWcp14_80C_DS	Mixed solution	86	0.04	3.1	4.0		No	5	0.08	-10.03	-9.61	8.56	8.38		Aragonite
UWcp14_8C_CA_5	Mixed solution	13	0.12	3.2	4.0	20	Yes	83	0.47	-9.95	-9.89	7.95	7.36		Calcite

UWcp14_20C_CA_13	Mixed solution	24	1.03	3.2	4.0	20	No	54	0.07	-10.28	-9.58	8.09	7.77		Calcite
UWcp14_50C_CA_9	Mixed solution	49	0.53	3.2	4.0	25	No	11	0.07	-10.31	-10.49	7.80	7.77	3.7	Calcite
UWcp14_70C_CA_4	Mixed solution	71	1.00	3.1	4.0	25	No	4	0.06	-10.34	-10.21	8.26	8.61	6.3	Calcite (62.6%), aragonite (38.5%)
<i>Molarity of CaCO₃ (mM)</i>															
UWcp14_30C_Z_1	Raft, filtered method	36	0.49		<12		Yes	9	0.1466			6.10	7.19		Aragonite
UWcp14_50C_Z_1	Raft, filtered method	50	0.83		<12		Yes	3	0.2169			6.40	7.82		Aragonite (91.7%), vaterite (8.1%)
UWcp14_4C_Z_3	Filtered	4	0.33		<13.2		Yes	68	0.0324			5.99	8.00		Calcite
UWcp14_20C_Z_15	Filtered	20	1.45		<11.2		Yes	20	0.3927			6.07	7.20		Calcite
UWcp14_20C_G_14	Filtered	21	0.49		<6.26		Yes	7	0.32	-10.52	-10.63	6.02	7.24		Calcite
UWcp14_20C_Z_2	Filtered	22	0.17		<10.3		Yes	30	0.4306			6.18	6.43		Calcite (92.9%), aragonite (7.1%)
UWcp14_50C_Z_2	Filtered	50	1		<13.2		Yes	9	0.2984			5.94	7.59		Aragonite

Table A2
Isotopic values of synthetic carbonates.

Sample	Precipitation Method	$\delta^{13}\text{C}$ vpdb ‰	$\delta^{13}\text{C}$ SD ‰	$\delta^{18}\text{O}$ calcite (considers aragonite and calcite CO ₂ -mineral fractionations)	vpdb ‰	$\delta^{18}\text{O}$ SD ‰	δ_{47} ‰	δ_{47} SD ‰	Δ_{47} ‰	Number of replicates digested in 90 °C (no acid correction) ^a	Number of replicates digested in 90 °C acid (n)	Δ_{47} SE ‰ (digested in 90 °C acid) ^b	Δ_{47} ‰ digested in 25 °C (no acid correction)	Number of replicates digested in 25 °C acid (n)	Δ_{47} SE ‰ (digested in 25 °C acid) ^c	1000ln α calcite water (smow)
UWcp14_4C_2	Actively degassed	-25.67	0.004	-7.54		0.06	-16.50	0.074	0.6724	3	3	0.014	0.7577	3	0.012	33.5
UWcp14_4C_4	Actively degassed	-23.52	0.017	-6.93		0.04	-13.82	0.037	0.6394	3	3	0.010		3		33.7
UWcp14_21C_1	Actively degassed	-18.56	0.162	-11.61		0.46	-13.67	0.630	0.6018	3	3	0.014	0.7049	3	0.012	29.6
UWcp14_40C_1	Actively degassed	-16.98	0.046	-15.19		0.10	-15.83	0.049	0.5366	3	3	0.014		3		26.0
UWcp14_50C_1	Actively degassed	-22.92	0.008	-16.19		0.11	-22.61	0.100	0.5586	3	3	0.014	0.6413	3	0.032	24.8
UWcp14_50C_2	Actively degassed	-18.26	0.045	-16.52		0.15	-18.44	0.134	0.5293	4	4	0.012		4		24.5
UWcp14_60C_2	Actively degassed	-12.55	0.014	-18.53		0.06	-14.93	0.095	0.5280	3	3	0.015		3		22.2
UWcp14_80C_1	Actively degassed	-21.13	0.215	-20.44		0.01	-25.26	0.209	0.4727	3	3	0.014	0.5576	3	0.012	20.3
UWcp14_80C_3	Actively degassed	-12.42	0.017	-20.16		0.17	-17.23	0.164	0.4584	3	3	0.015		3		20.4
UWcp14_24C_CA_1	Actively degassed	-21.04	0.014	-12.00		0.05	-16.50	0.041	0.5929	3	3	0.014		3		29.3
UWcp14_20C_CA_16	Actively degassed	-18.66	1.083	-11.09		0.11	-13.31	1.164	0.6555	4	4	0.014		4		29.9
UWcp14_50C_CA_3	Actively degassed	-15.27	0.024	-17.04		0.02	-16.07	0.055	0.5228	3	3	0.022		3		24.0
UWcp14_70C_CA_1	Actively degassed	-22.31	0.013	-20.46		0.06	-26.72	0.096	0.4753	4	4	0.014	0.6039	3	0.012	20.5
UWcp14_4C_3	Passively degassed	-21.76	0.671	-6.47		0.76	-11.63	0.212	0.6526	3	3	0.010		3		34.4
UWcp14_8C_2	Passively degassed	-15.08	0.045	-8.15		0.09	-6.86	0.094	0.6660	3	3	0.021		3		32.8
UWcp14_8C_3	Passively degassed	-16.46	0.023	-8.18		0.01	-8.25	0.010	0.6542	3	3	0.014		3		32.7
UWcp14_20C_9	Passively degassed	-20.92	0.115	-11.28		0.09	-15.64	0.169	0.6075	3	3	0.017	0.6867	4	0.010	29.8
UWcp14_20C_4	Passively degassed	-15.16	0.031	-10.41		0.05	-9.12	0.102	0.6083	4	4	0.020		4		30.9
UWcp14_20C_10	Passively degassed	-17.89	0.004	-11.36		0.04	-12.76	0.030	0.5968	3	3	0.014		3		29.9

UWcp14_50C_5	Passively degassed	-21.89	0.045	-15.85	0.08	-21.28	0.103	0.5339	2	0.017	0.6306	3	0.012	25.1
UWcp14_50C_3	Passively degassed	-13.58	0.003	-16.27	0.03	-13.61	0.033	0.5549	3	0.018				24.6
UWcp14_70C_4	Passively degassed	-17.67	0.101	-19.07	0.08	-20.53	0.176	0.4902	4	0.012				21.7
UWcp14_80C_2	Passively degassed	-6.16	0.025	-20.75	0.03	-11.07	0.011	0.4739	3	0.014				19.9
UWcp14_8C_CA_4	Passively degassed	-17.41	0.043	-8.17	0.06	-9.17	0.026	0.6462	2	0.013				32.9
UWcp14_20C_CA_5	Passively degassed	-18.55	0.015	-10.67	0.03	-12.69	0.047	0.6222	2	0.017				30.4
UWcp14_20C_CA_11	Passively degassed	-13.97	0.014	-11.26	0.00	-8.81	0.024	0.6268	3	0.014				29.8
UWcp14_50C_CA_10	Passively degassed	-18.42	0.106	-15.89	0.05	-18.20	0.164	0.5316	3	0.013				24.7
UWcp14_70C_CA_5	Passively degassed	-20.32	0.402	-19.40	0.21	-23.41	0.575	0.4746	3	0.014				21.4
UWcp14_35C_1	Passively degassed	-23.02	0.013	-14.93	0.03	-21.41	0.048	0.5876	3	0.014				26.2
UWcp14_50C_4	Passively degassed	-22.32	0.043	-16.02	0.24	-21.86	0.278	0.5521	3	0.015				25.0
UWcp14_60C_1	Passively degassed	-25.45	0.025	-18.03	0.10	-27.30	0.114	0.4918	3	0.015				22.8
UWcp14_3C_2	Mixed solution	-1.02	0.006	-8.78	0.03	6.11	0.028	0.6766	2	0.013				32.1
UWcp14_4C_1	Mixed solution	0.10	0.007	-8.70	0.01	7.26	0.014	0.6623	2	0.013	0.7915	3	0.018	31.6
UWcp14_4C_5	Mixed solution	-1.55	1.117	-7.62	0.41	6.80	0.683	0.6618	3	0.017				33.2
UWcp14_4C_6	Mixed solution	-0.01	0.273	-7.81	0.61	8.08	0.383	0.6906	2	0.020				33.3
UWcp14_8C_1	Mixed solution	0.03	0.009	-8.85	0.06	7.05	0.085	0.6746	4	0.009				32.0
UWcp14_8C_6	Mixed solution	0.40	0.018	-8.88	0.02	7.36	0.043	0.6817	3	0.016				32.2
UWcp14_20C_DS	Mixed solution	0.60	0.074	-12.18	0.01	4.06	0.070	0.6312	3	0.010				28.5
UWcp14_50C_7	Mixed solution	-0.29	0.007	-17.69	0.05	-2.16	0.054	0.5325	3	0.014				22.8
UWcp14_50C_8	Mixed solution	-0.89	0.002	-16.34	0.02	-1.32	0.037	0.5488	3	0.015				24.5
UWcp14_50C_DS	Mixed solution	-0.15	0.074	-17.34	0.03	-2.16	0.093	0.5301	3	0.010				23.3
UWcp14_50C_DS2	Mixed solution	0.40	0.079	-16.82	0.03	-1.08	0.092	0.5295	3	0.013				23.9

(continued on next page)

Table A2 (continued)

Sample	Precipitation Method	$\delta^{13}\text{C}$ vpdb ‰	$\delta^{13}\text{C}$ SD ‰	$\delta^{18}\text{O}$ calcite (considers aragonite and calcite CO ₂ -mineral fractionations)	$\delta^{18}\text{O}$ SD ‰	δ_{47} ‰	δ_{47} SD ‰	Δ_{47} ‰	Δ_{47} SD ‰	Number of replicates digested in 90 °C (no acid correction) ^a	Number of replicates digested in 90 °C acid (n)	Δ_{47} SE ‰ (digested in 90 °C acid) ^b	Δ_{47} ‰ digested in 25 °C (no acid correction)	Number of replicates digested in 25 °C acid (n)	Δ_{47} SE ‰ (digested in 25 °C acid) ^c	1000ln α calcite water (smow)
UWcp14_70C_DS2	Mixed solution	0.92	0.067	-19.05	0.18	-3.29	0.155	0.4706		3		0.015	0.6041	5	0.010	21.4
UWcp14_70C_2	Mixed solution	1.57	0.020	-19.48	0.10	-2.52	0.144	0.5258		3		0.014				20.7
UWcp14_80C_DS	Mixed solution	0.75	0.046	-20.36	0.14	-4.84	0.119	0.4567		3		0.019				19.7
UWcp14_8C_CA_5	Mixed solution	-1.82	1.413	-9.14	0.32	4.95	1.040	0.6681		3		0.010				31.4
UWcp14_20C_CA_13	Mixed solution	-2.03	0.500	-12.01	0.15	1.69	0.321	0.6241		3		0.010	0.7077	2	0.014	28.5
UWcp14_50C_CA_9	Mixed solution	-0.24	0.073	-16.76	0.03	-1.62	0.097	0.5453		3		0.010				24.0
UWcp14_70C_CA_4	Mixed solution	-0.29	0.041	-19.83	0.04	-4.41	0.047	0.4914		3		0.014	0.5685	2	0.018	20.7
UWcp14_30C_Z_1	Raft, filtered method	-23.26	0.350	-12.32	0.63	-19.40	0.292	0.5486		2		0.020				28.8
UWcp14_50C_Z_1	Raft, filtered method	-22.99	0.007	-15.51	0.08	-22.42	0.069	0.5336		2		0.020				25.3
UWcp14_4C_Z_3	Filtered	-25.32	0.942	-8.07	0.39	-16.61	1.293	0.6689		3		0.016				33.2
UWcp14_20C_Z_15	Filtered	-22.68	0.008	-11.03	0.11	-17.11	0.123	0.6482		5		0.013				30.2
UWcp14_20C_Z_2	Filtered	-23.74	0.949	-11.43	0.10	-18.57	0.831	0.6261		3		0.016				29.8
UWcp14_20C_G_14	Filtered	-24.70	0.011	-11.62	0.01	-19.80	0.014	0.6068		2		0.013				29.5
UWcp14_50C_Z_2	Filtered	-24.08	0.625	-15.49	0.06	-23.43	0.517	0.5406		2		0.020				25.1
Chicken egg shell		-0.23	0.055	-7.41	0.06	8.57	0.10	0.5760		4		0.014				

^a Values calculated with Brand et al. (2010) ¹⁷O correction parameters.

^b Where the standard deviation of D47 of the sample was lower than the long term standard deviation of C64, SD of C64 was used to calculate SE of the sample for the first reference frame, C64 SD = 0.024 for the second reference frame, C64 SD = 0.08 for the third reference frame, C64 SD = 0.028.

^c Where the standard deviation of D47 of the sample was lower than the long term standard deviation of C64 reacted at 25 °C (SD = 0.020), SD of C64 was used to calculate SE for the sample.

Table A3
Isotopic Values of Synthetic Carbonates, processed with Santrock et al. (1985) values.

Sample	Precipitation Method	$\delta^{13}\text{C}$ vpdb ‰	$\delta^{13}\text{C}$ SD ‰	$\delta^{18}\text{O}$ calcite vpdb ‰ (considers aragonite and calcite CO_2 -mineral fractionations)	$\delta^{18}\text{O}$ SD ‰	δ_{47} ‰	δ_{47} SD ‰	Δ_{47} ‰ digested in 90 °C (no acid correction) ^a	Number of replicates digested in 90 °C acid (n)	Δ_{47} SE ‰ (digested in 90 °C acid) ^b	Δ_{47} ‰ digested in 25 °C (no acid correction)	Number of replicates digested in 25 °C acid (n)	Δ_{47} SE ‰ (digested in 25 °C acid) SE ^c
UWcp14_4C_2	Actively degassed	-25.67	0.00	-7.56	0.06	-16.50	0.07	0.6403	3	0.014	0.7265	3	0.012
UWcp14_4C_4	Actively degassed	-23.52	0.02	-6.94	0.04	-13.82	0.04	0.6114	3	0.010			
UWcp14_21C_1	Actively degassed	-18.50	0.21	-11.61	0.46	-13.67	0.63	0.5872	3	0.014	0.6867	3	0.012
UWcp14_40C_1	Actively degassed	-16.98	0.05	-15.19	0.10	-15.83	0.05	0.5247	3	0.014			
UWcp14_50C_1	Actively degassed	-22.91	0.01	-16.10	0.20	-22.61	0.10	0.5365	3	0.014	0.6168	3	0.032
UWcp14_50C_2	Actively degassed	-18.25	0.04	-16.52	0.15	-18.44	0.13	0.5153	4	0.012			
UWcp14_60C_2	Actively degassed	-12.56	0.01	-18.53	0.06	-14.93	0.10	0.5242	3	0.015			
UWcp14_80C_1	Actively degassed	-21.13	0.21	-20.44	0.01	-25.26	0.21	0.4538	3	0.014	0.5372	3	0.012
UWcp14_80C_3	Actively degassed	-12.44	0.02	-20.56	0.17	-17.23	0.16	0.4524	3	0.015			
UWcp14_24C_CA_1	Actively degassed	-21.11	0.01	-12.03	0.14	-16.50	0.04	0.5765	3	0.014			
UWcp14_20C_CA_16	Actively degassed	-18.65	1.08	-11.10	0.11	-13.31	1.16	0.6408	4	0.014			
UWcp14_50C_CA_3	Actively degassed	-15.28	0.02	-17.04	0.02	-16.07	0.05	0.5140	3	0.022			
UWcp14_70C_CA_1	Actively degassed	-22.31	0.01	-20.46	0.06	-26.72	0.10	0.4544	4	0.014	0.5450	3	0.012
UWcp14_4C_3	Passively degassed	-21.76	0.67	-6.48	0.76	-11.63	0.21	0.6277	3	0.010			
UWcp14_8C_2	Passively degassed	-15.07	0.05	-8.17	0.09	-6.86	0.09	0.6533	3	0.021			
UWcp14_8C_3	Passively degassed	-16.46	0.02	-8.20	0.01	-8.25	0.01	0.6391	3	0.014			
UWcp14_20C_9	Passively degassed	-20.90	0.11	-11.28	0.09	-15.64	0.17	0.5882	3	0.017	0.6667	4	0.010

(continued on next page)

Table A3 (continued)

Sample	Precipitation Method	$\delta^{13}\text{C}$ vpdb ‰	$\delta^{13}\text{C}$ SD ‰	$\delta^{18}\text{O}$ calcite vpdb ‰ (considers aragonite and calcite CO_2 -mineral fractionations)	$\delta^{18}\text{O}$ SD ‰	δ_{47} ‰	δ_{47} SD ‰	Δ_{47} ‰ digested in 90 °C (no acid correction) ^a	Number of replicates digested in 90 °C acid (n)	Δ_{47} SE ‰ (digested in 90 °C acid) ^b	Δ_{47} ‰ digested in 25 °C (no acid correction)	Number of replicates digested in 25 °C acid (n)	Δ_{47} SE ‰ (digested in 25 °C acid) SE ^c
UWcp14_20C_4	Passively degassed	-15.16	0.03	-10.41	0.05	-9.12	0.10	0.5994	4	0.020			
UWcp14_20C_10	Passively degassed	-17.88	0.00	-11.36	0.04	-12.76	0.03	0.5830	3	0.014			
UWcp14_50C_5	Passively degassed	-21.87	0.06	-15.88	0.07	-21.31	0.13	0.5060	2	0.017	0.6080	3	0.012
UWcp14_50C_3	Passively degassed	-13.59	0.00	-16.27	0.03	-13.61	0.03	0.5492	3	0.018			
UWcp14_70C_4	Passively degassed	-17.68	0.10	-19.10	0.09	-20.53	0.18	0.4773	4	0.012			
UWcp14_80C_2	Passively degassed	-6.20	0.02	-20.75	0.03	-11.07	0.01	0.4808	3	0.014			
UWcp14_8C_CA_4	Passively degassed	-17.41	0.04	-8.19	0.06	-9.17	0.03	0.6294	2	0.013			
UWcp14_20C_CA_5	Passively degassed	-18.54	0.01	-10.68	0.03	-12.69	0.05	0.6072	2	0.017			
UWcp14_20C_CA_11	Passively degassed	-13.97	0.01	-11.26	0.00	-8.82	0.02	0.6156	3	0.014			
UWcp14_50C_CA_10	Passively degassed	-18.43	0.11	-15.94	0.05	-18.20	0.16	0.5140	3	0.013			
UWcp14_70C_CA_5	Passively degassed	-20.55	0.05	-19.40	0.21	-23.41	0.58	0.4568	3	0.014			
UWcp14_35C_1	Passively degassed	-23.01	0.01	-14.93	0.03	-21.41	0.05	0.5647	3	0.014			
UWcp14_50C_4	Passively degassed	-22.31	0.04	-16.02	0.24	-21.86	0.28	0.5306	3	0.015			
UWcp14_60C_1	Passively degassed	-25.44	0.03	-18.03	0.10	-27.30	0.00	0.4647	3	0.015			
UWcp14_3C_2	Mixed solution	-1.00	0.01	-8.80	0.03	6.11	0.03	0.6893	2	0.013			
UWcp14_4C_1	Mixed solution	0.11	0.01	-8.72	0.01	7.26	0.01	0.6771	2	0.013	0.8047	3	0.018
UWcp14_4C_5	Mixed solution	-1.54	1.12	-7.63	0.41	6.80	0.68	0.6736	3	0.017			
UWcp14_4C_6	Mixed solution	0.00	0.27	-7.83	0.61	8.08	0.27	0.7088	2	0.020			
UWcp14_8C_1	Mixed solution	0.04	0.01	-8.87	0.06	7.05	0.09	0.6893	4	0.009			
UWcp14_8C_6	Mixed solution	0.41	0.02	-8.89	0.05	7.40	0.08	0.7006	3	0.016			

UWcp14_20C_DS	Mixed solution	0.60	0.07	-12.21	0.01	4.06	0.07	0.6471	3	0.010			
UWcp14_50C_7	Mixed solution	-0.33	0.01	-17.69	0.05	-2.16	0.05	0.5506	3	0.014			
UWcp14_50C_8	Mixed solution	-0.92	0.00	-16.33	0.02	-1.32	0.04	0.5658	3	0.015			
UWcp14_50C_DS	Mixed solution	-0.15	0.07	-17.39	0.03	-2.16	0.09	0.5455	3	0.010			
UWcp14_50C_DS2	Mixed solution	0.40	0.08	-16.87	0.03	-1.08	0.09	0.5458	3	0.013			
UWcp14_70C_DS2	Mixed solution	0.92	0.07	-19.11	0.19	-3.29	0.16	0.4882	3	0.015	0.5957	5	0.010
UWcp14_70C_2	Mixed solution	1.52	0.02	-19.48	0.10	-2.52	0.14	0.5459	3	0.014			
UWcp14_80C_DS	Mixed solution	0.75	0.05	-20.43	0.14	-4.84	0.12	0.4742	3	0.019			
UWcp14_8C_CA_5	Mixed solution	-1.80	1.41	-9.17	0.32	4.95	1.04	0.6794	3	0.010			
UWcp14_20C_CA_13	Mixed solution	-2.03	0.50	-12.05	0.16	1.69	0.32	0.6354	3	0.010	0.7183	2	0.014
UWcp14_50C_CA_9	Mixed solution	-0.24	0.07	-16.81	0.03	-1.62	0.10	0.5604	3	0.010			
UWcp14_70C_CA_4	Mixed solution	-0.33	0.04	-19.83	0.04	-4.41	0.05	0.5096	3	0.014	0.5828	2	0.018
UWcp14_30C_Z_1	Raft, filtered method	-23.25	0.35	-12.63	0.58	-19.40	0.29	0.5257	2	0.020			
UWcp14_50C_Z_1	Raft, filtered method	-22.99	0.00	-15.81	0.01	-22.70	0.07	0.5114	2	0.020			
UWcp14_4C_Z_3	Filtered	-25.30	0.95	-8.08	0.39	-16.61	1.29	0.6419	3	0.016			
UWcp14_20C_Z_15	Filtered	-23.17	0.01	-10.97	0.11	-17.53	0.12	0.6336	5	0.013			
UWcp14_20C_Z_2	Filtered	-23.73	0.95	-11.44	0.10	-18.57	0.83	0.6022	3	0.016			
UWcp14_20C_G_14	Filtered	-24.72	0.01	-11.65	0.01	-19.80	0.01	0.5770	2	0.013			
UWcp14_50C_Z_2	Filtered	-24.08	0.62	-15.79	0.06	-23.43	0.52	0.5164	2	0.020			
Chicken egg shell		-0.26	0.06	-7.41	0.06	8.57	0.10	0.5940	4	0.014			

^a Values calculated with [Santrock et al. \(1985\)](#) ¹⁷O correction parameters.

^b Where the standard deviation of D47 of the sample was lower than the long term standard deviation of C64, SD of C64 was used to calculate SE of the sample for the first reference frame, C64 SD = 0.024 for the second reference frame, C64 SD = 0.0*8 for the third reference frame, C64 SD = 0.028.

^c Where the standard deviation of D47 of the sample was lower than the long term standard deviation of C64 reacted at 25 °C (SD = 0.020), SD of C64 was used to calculate SE for the sample.

REFERENCES

- Affek H. P. (2012) Clumped isotope palaeothermometry: principles, applications, and challenges. *Paleontol. Soc. Publ.* **18**, 101–114.
- Affek H. P. (2013) Clumped isotopic equilibrium and the rate of isotope exchange between CO₂ and water. *Am. J. Sci.* **313**, 309–325.
- Affek H. P. and Eiler J. M. (2006) Abundance of mass 47 CO₂ in urban air, car exhaust, and human breath. *Geochim. Cosmochim. Acta* **70**, 1–12.
- Affek H. P. and Zaarur S. (2014) Kinetic isotope effect in CO₂ degassing: insight from clumped and oxygen isotopes in laboratory precipitation experiments. *Geochim. Cosmochim. Acta* **143**, 319–330.
- Affek H. P., Matthews A., Ayalon A., Bar-Matthews M., Burstyn Y., Zaarur S. and Zilberman T. (2014) Accounting for kinetic isotope effects in Soreq Cave (Israel) speleothems. *Geochim. Cosmochim. Acta* **143**, 303–318.
- Bernasconi S. M., Hu B., Wacker U., Fiebig J., Breitenbach S. F. M. and Rutz T. (2013) Background effects on Faraday collectors in gas-source mass spectrometry and implications for clumped isotope measurements. *Rapid Commun. Mass Spectrom.* **27**, 603–612.
- Brand W. A., Assonov S. S. and Coplen T. B. (2010) Correction for the 17O interference in $\delta^{13}\text{C}$ measurements when analyzing CO₂ with stable isotope mass spectrometry (IUPAC Technical Report). *Pure Appl. Chem.* **82**, 1719–1733.
- Breecker D. O., Sharp Z. D. and McFadden L. D. (2009) Seasonal bias in the formation and stable isotopic composition of pedogenic carbonate in modern soils from central New Mexico, USA. *Bull. Geol. Soc. Am.* **121**, 630–640.
- Burgener L., Huntington K. W., Hoke G. D., Schauer A., Ringham M. C., Latorre C. and Díaz F. P. (2016) Variations in soil carbonate formation and seasonal bias over >4 km of relief in the western Andes (30°S) revealed by clumped isotope thermometry. *Earth Planet. Sci. Lett.* **441**, 188–199.
- Came R. E., Brand U. and Affek H. P. (2014) Clumped isotope signatures in modern brachiopod carbonate. *Chem. Geol.* **377**, 20–30.
- Colman, A.S., and Olack, G. (2015). Resolving the dependency of Δ_{47} thermometers on acid digestion temperature. Abstract PP23D-01 presented at AGU Fall Meeting, San Francisco, 14–18 Dec.
- Coplen T. B. (2007) Calibration of the calcite–water oxygen-isotope geothermometer at Devils Hole, Nevada, a natural laboratory. *Geochim. Cosmochim. Acta* **71**, 3948–3957.
- Daëron M., Guo W., Eiler J., Genty D., Blamart D., Boch R., Drysdale R., Maire R., Wainer K. and Zanchetta G. (2011) 13C18O clumping in speleothems: observations from natural caves and precipitation experiments. *Geochim. Cosmochim. Acta* **75**, 3303–3317.
- Daëron M., Blamart D., Peral M. and Affek H. P. (2016) Absolute isotopic abundance ratios and the accuracy of Δ_{47} measurements. *Chem. Geol.* **442**, 83–96.
- Defliese W. F., Hren M. T. and Lohmann K. C. (2015) Compositional and temperature effects of phosphoric acid fractionation on Δ_{47} analysis and implications for discrepant calibrations. *Chem. Geol.* **396**, 51–60.
- DeLuca V., Vullo D., Scozzafava A., Carginale V., Rossi M. and Capasso C. (2013) An α -carbonic anhydrase from the thermophilic bacterium Sulphurihydrogenibium azorense is the fastest enzyme known for the CO₂ hydration reaction. *Bioorg. Med. Chem.* **21**, 1465–1469.
- Dennis K. J. and Schrag D. P. (2010) Clumped isotope thermometry of carbonates as an indicator of diagenetic alteration. *Geochim. Cosmochim. Acta* **74**, 4110–4122.
- Dennis K. J., Affek H. P., Passey B. H., Schrag D. P. and Eiler J. M. (2011) Defining an absolute reference frame for “clumped” isotope studies of CO₂. *Geochim. Cosmochim. Acta* **75**, 7117–7131.
- Eagle R. A., Schauble E. A., Tripathi A. K., Tütken T., Hulbert R. C. and Eiler J. M. (2010) Body temperatures of modern and extinct vertebrates from 13C–18O bond abundances in bioapatite. *Proc. Natl. Acad. Sci. U.S.A.* **107**, 10377–10382.
- Eagle R. A., Eiler J. M., Tripathi A. K., Ries J. B., Freitas P. S., Hiebenthal C., Wanamaker A. D., Taviani M., Elliot M., Marensi S., Nakamura K., Ramirez P. and Roy K. (2013) The influence of temperature and seawater carbonate saturation state on 13C–18O bond ordering in bivalve mollusks. *Biogeosciences* **10**, 4591–4606.
- Eagle R. A., Enriquez M., Grillet-Tinner G., Pérez-Huerta A., Hu D., Tütken T., Montanari S., Loyd S. J., Ramirez P., Tripathi A. K., John M. J., Cerling T. E., Chiappe L. M. and Eiler J. M. (2015) Isotopic ordering in eggshells reflects body temperatures and suggests two differing thermophysiology in two Cretaceous dinosaurs. *Nat. Commun.* **6**, 1–11.
- Eiler J. M. (2007) “Clumped-isotope” geochemistry—The study of naturally-occurring, multiply-substituted isotopologues. *Earth Planet. Sci. Lett.* **262**, 309–327.
- Eiler J. M. (2011) Paleoclimate reconstruction using carbonate clumped isotope thermometry. *Quat. Sci. Rev.* **30**, 3575–3588.
- Eiler J. M. and Schauble E. (2004) $^{18}\text{O}^{13}\text{C}^{16}\text{O}$ in Earth’s atmosphere. *Geochim. Cosmochim. Acta* **68**, 4767–4777.
- Eiler J. M., Clog M., Magyar P., Piasecki A., Sessions A., Stolper D., Deerberg M., Schlueter H.-J. and Schwieters J. (2013) A high-resolution gas-source isotope ratio mass spectrometer. *Int. J. Mass Spectrom.* **335**, 45–56.
- Eiler J. M., Bergquist B., Bourg I., Cartigny P., Farquhar J., Gagnon A., Guo W., Halevy I., Hofmann A., Larson T. E., Levin N., Schauble E. A. and Stolper D. (2014) Frontiers of stable isotope geoscience. *Chem. Geol.* **372**, 119–143.
- Falk E. S., Guo W., Paukert A. N., Matter J. M., Mervine E. M. and Kelemen P. B. (2016) Controls on the stable isotope compositions of travertine from hyperalkaline springs in Oman: insights from clumped isotope measurements. *Geochim. Cosmochim. Acta* **192**, 1–28.
- Fenter P. and Sturchio N. C. (2004) Mineral–water interfacial structures revealed by synchrotron X-ray scattering. *Prog. Surf. Sci.* **77**, 171–258.
- Fenter P. and Sturchio N. C. (2012) Calcite (104)–water interface structure, revisited. *Geochim. Cosmochim. Acta* **97**, 58–69.
- Fenter P., Kerisit S., Raiteri P. and Gale J. D. (2013) Is the calcite–water interface understood? Direct comparisons of molecular dynamics simulations with specular X-ray reflectivity data. *J. Phys. Chem. C* **117**, 5028–5042.
- Fernandez A., Tang J. and Rosenheim B. E. (2014) Siderite “clumped” isotope thermometry: a new paleoclimate proxy for humid continental environments. *Geochim. Cosmochim. Acta* **126**, 411–421.
- Fiebig J., Hofmann S., Löffler N., Lüdecke T., Methner K. and Wacker U. (2015) Slight pressure imbalances can affect accuracy and precision of dual inlet-based clumped isotope analysis. *Isotopes Environ Health Stud* **6016**, 1–17.
- Geissbühler P., Fenter P., DiMasi E., Srajer G., Sorensen L. B. and Sturchio N. C. (2004) Three-dimensional structure of the calcite–water interface by surface X-ray scattering. *Surf. Sci.* **573**, 191–203.

- Ghosh P., Adkins J., Affek H., Balta B., Guo W., Schauble E. A., Schrag D. and Eiler J. M. (2006) ^{13}C – ^{18}O bonds in carbonate minerals: a new kind of paleothermometer. *Geochim. Cosmochim. Acta* **70**, 1439–1456.
- Ghosh P., Eiler J., Campana S. E. and Feeney R. F. (2007) Calibration of the carbonate “clumped isotope” paleothermometer for otoliths. *Geochim. Cosmochim. Acta* **71**, 2736–2744.
- Grauel A.-L., Schmid T. W., Hu B., Bergami C., Capotondi L., Zhou L. and Bernasconi S. M. (2013) Calibration and application of the “clumped isotope” thermometer to foraminifera for high-resolution climate reconstructions. *Geochim. Cosmochim. Acta* **108**, 125–140.
- Guo W. (2009) *Carbonate Clumped Isotope Thermometry: Application to Carbonaceous Chondrites & Effects of Kinetic Isotope Fractionations* (PhD Thesis). California Institute of Technology.
- Guo W., Mosenfelder J. L., Goddard W. A. and Eiler J. M. (2009) Isotopic fractionations associated with phosphoric acid digestion of carbonate minerals: insights from first-principles theoretical modeling and clumped isotope measurements. *Geochim. Cosmochim. Acta* **73**, 7203–7225.
- Gupta P., Noone D., Galewsky J., Sweeney C. and Vaughn B. H. (2009) Demonstration of high-precision continuous measurements of water vapor isotopologues in laboratory and remote field deployments using wavelength-scanned and cavity ring-down spectroscopy (WS-CRDS) technology. *Rapid Commun. Mass Spectrom.* **23**, 2534–2542.
- He B., Olack G. A. and Colman A. S. (2012) Pressure baseline correction and high-precision CO_2 clumped-isotope (Δ_{47}) measurements in bellows and micro-volume modes. *Rapid Commun. Mass Spectrom.* **26**, 2837–2853.
- Henkes G. A., Passey B. H., Wanamaker A. D., Grossman E. L., Ambrose W. G. and Carroll M. L. (2013) Carbonate clumped isotope compositions of modern marine mollusk and brachiopod shells. *Geochim. Cosmochim. Acta* **106**, 307–325.
- Hill P. S., Tripathi A. K. and Schauble E. A. (2014) Theoretical constraints on the effects of pH, salinity, and temperature on clumped isotope signatures of dissolved inorganic carbon species and precipitating carbonate minerals. *Geochim. Cosmochim. Acta* **125**, 610–652.
- Hren M. T. and Sheldon N. D. (2012) Temporal variations in lake water temperature: paleoenvironmental implications of lake carbonate $\delta^{18}\text{O}$ and temperature records. *Earth Planet. Sci. Lett.* **337–338**, 77–84.
- Huntington K. W., Eiler J. M., Affek H. P., Guo W., Bonifacie M., Yeung L. Y., Thiagarajan N., Passey B., Tripathi A., Daëron M. and Came R. (2009) Methods and limitations of “clumped” CO_2 isotope (Δ_{47}) analysis by gas-source isotope ratiomass spectrometry. *J. Mass Spectrom.* **44**, 1318–1329.
- Huntington K. W. and Lechler A. R. (2015) Carbonate clumped isotope thermometry in continental tectonics. *Tectonophysics* **647–648**, 1–20.
- Kele S., Breitenbach S. F. M., Capezuoli E., Nele Meckler A., Ziegler M., Millan I. M., Kluge T., Deák J., Hanselmann K., John C. M., Yan H., Liu Z. and Bernasconi S. M. (2015) Temperature dependence of oxygen- and clumped isotope fractionation in carbonates: a study of travertines and tufas in the 6–95 °C temperature range. *Geochim. Cosmochim. Acta* **168**, 172–192.
- Kim S.-T. and O’Neil J. R. (1997) Equilibrium and nonequilibrium oxygen isotope effects in synthetic carbonates. *Geochim. Cosmochim. Acta* **61**, 3461–3475.
- Kluge T. and Affek H. P. (2012) Quantifying kinetic fractionation in Bunker Cave speleothems using Δ_{47} . *Quat. Sci. Rev.* **49**, 82–94.
- Kluge T., Affek H. P., Marx T., Aeschbach-Hertig W., Riechelmann D. F. C., Scholz D., Riechelmann S., Immenhauser A., Richter D. K., Fohlmeister J., Wackerbarth A., Mangini A. and Spötl C. (2013) Reconstruction of drip-water $\delta^{18}\text{O}$ based on calcite oxygen and clumped isotopes of speleothems from Bunker Cave (Germany). *Clim. Past* **9**, 377–391.
- Kluge T., Affek H. P., Dublyansky Y. and Spötl C. (2014) Devils hole paleotemperatures and implications for oxygen isotope equilibrium fractionation. *Earth Planet. Sci. Lett.* **400**, 251–260.
- Kluge T., John C. M., Jourdan A.-L., Davis S. and Crawshaw J. (2015) Laboratory calibration of the calcium carbonate clumped isotope thermometer in the 25–250 °C temperature range. *Geochim. Cosmochim. Acta* **157**, 213–227.
- McCrea J. M. (1950) On the isotopic chemistry of carbonates and a paleotemperature scale. *J. Chem. Phys.* **18**, 849–857.
- Mickler P. J., Banner J. L., Stern L., Asmerom Y., Edwards R. L. and Ito E. (2004) Stable isotope variations in modern tropical speleothems: evaluating equilibrium vs. kinetic isotope effects. *Geochim. Cosmochim. Acta* **68**, 4381–4393.
- Olack G. and Colman A. (2016) Influence of ^{17}O correction parameters on calculation and calibration of Δ_{47} . Abstract presented at Goldschmidt, Yokohama, Japan, 26 June–1 July.
- Passey B. H. and Henkes G. A. (2012) Carbonate clumped isotope bond reordering and geospeedometry. *Earth Planet. Sci. Lett.* **351–352**, 223–236.
- Passey B. H., Levin N. E., Cerling T. E., Brown F. H. and Eiler J. M. (2010) High-temperature environments of human evolution in East Africa based on bond ordering in paleosol carbonates. *Proc. Natl. Acad. Sci. U.S.A.* **107**, 11245–11249.
- Petruzzo D. A., Young E. D. and Runnegar B. N. (2014) Implications of high-precision measurements of ^{13}C – ^{18}O bond ordering in CO_2 for thermometry in modern bivalved mollusk shells. *Geochim. Cosmochim. Acta* **142**, 400–410.
- Petersen S. V., Winkelstern I. Z., Lohmann K. C. and Meyer K. W. (2016) The effects of PorapakTM trap temperatures on $\delta^{18}\text{O}$, $\delta^{13}\text{C}$, and Δ_{47} values in preparing samples for clumped isotope analysis. *Rapid Commun. Mass Spectrom.* **30**, 199–208.
- Quade J., Garzione C. and Eiler J. (2007) Paleoelevation Reconstruction using Pedogenic Carbonates. *Rev. Miner. Geochem.* **66**, 53–87.
- Quade J., Eiler J., Daëron M. and Achyuthan H. (2013) The clumped isotope geothermometer in soil and paleosol carbonate. *Geochim. Cosmochim. Acta* **105**, 92–107.
- Randall W. C. and Hiestand W. A. (1939) Panting and temperature regulation in chicken. *Am. J. Physiol.* **127**, 761–767.
- Reddy M. M. (1995) Carbonate precipitation in Pyramid Lake, Nevada. In *Mineral Scale Formation and Inhibition*. Plenum Press, NY, pp. 21–32.
- Ross S. M. (2003) Peirce’s criterion for the elimination of suspect experimental data. *J. Eng. Technol.* **20**, 1–12.
- Saenger C., Affek H. P., Felis T., Thiagarajan N., Lough J. M. and Holcomb M. (2012) Carbonate clumped isotope variability in shallow water corals: temperature dependence and growth-related vital effects. *Geochim. Cosmochim. Acta* **99**, 224–242.
- Santrock J., Studley S. A. and Hayes J. M. (1985) Isotopic analyses based on the mass spectrum of carbon dioxide. *Anal. Chem.* **57**, 1444–1448.
- Schauble E. A., Ghosh P. and Eiler J. M. (2006) Preferential formation of ^{13}C – ^{18}O bonds in carbonate minerals, estimated using first-principles lattice dynamics. *Geochim. Cosmochim. Acta* **70**, 2510–2529.
- Schauer A. J., Kelson J., Saenger C. and Huntington K. W. (2016) Choice of ^{17}O correction affects clumped isotope (Δ_{47}) values of CO_2 measured with mass spectrometry. *Rapid Commun. Mass Spectrom.* <http://dx.doi.org/10.1002/rcm.7743>.

- Tang J., Dietzel M., Fernandez A., Tripathi A. K. and Rosenheim B. E. (2014) Evaluation of kinetic effects on clumped isotope fractionation (Δ_{47}) during inorganic calcite precipitation. *Geochim. Cosmochim. Acta* **134**, 120–136.
- Thiagarajan N., Adkins J. and Eiler J. (2011) Carbonate clumped isotope thermometry of deep-sea corals and implications for vital effects. *Geochim. Cosmochim. Acta* **75**, 4416–4425.
- Tobin T. S., Schauer A. J. and Lewarch E. (2011) Alteration of micromilled carbonate $\delta^{18}\text{O}$ during Kiel Device analysis. *Rapid Commun. Mass Spectrom.* **25**, 2149–2152.
- Tripathi A. K., Eagle R. A., Thiagarajan N., Gagnon A. C., Bauch H., Halloran P. R. and Eiler J. M. (2010) ^{13}C – ^{18}O isotope signatures and “clumped isotope” thermometry in foraminifera and coccoliths. *Geochim. Cosmochim. Acta* **74**, 5697–5717.
- Tripathi A. K., Hill P. S., Eagle R. A., Mosenfelder J. L., Tang J., Schauble E. A., Eiler J. M., Zeebe R. E., Uchikawa J., Coplen T. B., Ries J. B. and Henry D. (2015) Beyond temperature: clumped isotope signatures in dissolved inorganic carbon species and the influence of solution chemistry on carbonate mineral composition. *Geochim. Cosmochim. Acta* **166**, 344–371.
- Uchikawa J. and Zeebe R. E. (2012) The effect of carbonic anhydrase on the kinetics and equilibrium of the oxygen isotope exchange in the CO_2 – H_2O system: implications for $\delta^{18}\text{O}$ vital effects in biogenic carbonates. *Geochim. Cosmochim. Acta* **95**, 15–34.
- Wacker U., Fiebig J. and Schoene B. R. (2013) Clumped isotope analysis of carbonates: comparison of two different acid digestion techniques. *Rapid Commun. Mass Spectrom.* **27**, 1631–1642.
- Wacker U., Fiebig J., Tödter J., Schöne B. R., Bahr A., Friedrich O., Tütken T., Gischler E. and Joachimski M. M. (2014) Empirical calibration of the clumped isotope paleothermometer using calcites of various origins. *Geochim. Cosmochim. Acta* **141**, 127–144.
- Wang X., Conway W., Burns R., McCann N. and Maeder M. (2009) Comprehensive Study of the Hydration and Dehydration Reactions of Carbon Dioxide in Aqueous Solution. *J. Phys. Chem. A* **114**, 1734–1740.
- Watkins J. M. and Hunt J. D. (2015) A process-based model for non-equilibrium clumped isotope effects in carbonates. *Earth Planet. Sci. Lett.* **432**, 152–165.
- Watkins J. M., Nielsen L. C., Ryerson F. J. and DePaolo D. J. (2013) The influence of kinetics on the oxygen isotope composition of calcium carbonate. *Earth Planet. Sci. Lett.* **375**, 349–360.
- Watkins J. M., Hunt J. D., Ryerson F. J. and DePaolo D. J. (2014) The influence of temperature, pH, and growth rate on the $\delta^{18}\text{O}$ composition of inorganically precipitated calcite. *Earth Planet. Sci. Lett.* **404**, 332–343.
- York D., Evensen N. M., Martínez M. L. and De Basabe Delgado J. (2004) Unified equations for the slope, intercept, and standard errors of the best straight line. *Am. J. Phys.* **72**, 367.
- Zaarur S., Affek H. P. and Brandon M. T. (2013) A revised calibration of the clumped isotope thermometer. *Earth Planet. Sci. Lett.* **382**, 47–57.
- Zeebe R. E. (1999) An explanation of the effect of seawater carbonate concentration on foraminiferal oxygen isotopes. *Geochim. Cosmochim. Acta* **63**, 2001–2007.
- Zeebe R. E. (2007) An expression for the overall oxygen isotope fractionation between the sum of dissolved inorganic carbon and water. *Geochem., Geophys. Geosyst.* **8**, 1–7.

Associate editor: Hagit Affek